(A)



(B)



(C)



(D)



(E)

Fig. 3. Schematic illustration of WINA function in VDR-mediated gene regulations with 10-regulatory complexes.

ligand-induced TRAP220 and TIF2 occupancy was cyclic (data not shown) as expected from previous reports [20].

As the VDR/RXR heterodimer also represses transcription in a ligand-dependent manner through negative VDRE (nVDRE), the action of WSTF in the ligand-induced transrepression was examined in a naturally occurring nVDRE in human 25-hydroxyvitamin D3 1α-hydroxylase [1α(OH)ase] [22]. ChIP analysis uncovered that VDR and WINAC appear to land on the nVDRE in a ligand-independent manner, while ligand-induced, but cyclic (data not shown) recruitments of N-CoR and HDAC2 were observed. Ligand-dependent repression was exaggerated by WSTF overexpression, but attenuated again by WSTF-RNAi expression (Fig. 2B). Thus, it is likely that WINAC association with VDR facilitates targeting of a putative co-repressor complex to the nVDRE. Thus, these findings point out that WINAC rearranges the nucleosome array around the positive and negative VDREs, thereby facilitating the co-regulatory complexes accessible to VDR for further transcription control.

## 5. Promoter targeting of VDR by WINAC, with cooperation of WINAC with the co-regulator complexes

From our ChIP analysis, VDR appears to be selectively targeted through WINAC to the promoters without ligand-induced activation of VDR function or following recruitment of co-regulator complexes. This ligand-independent association with the target promoter in VDR is unexpectedly distinct from the ligand-induced promoter targeting of many steroid receptors [20,21]. It is possible to speculate that the other non-steroidal receptors like RAR, RXR and TR may associate with their target promoters without ligand binding, and unidentified chromatin remodeling complexes may assist the promoter targeting.

As HAT and HDAC complexes appears not to associate with unliganded VDR, WINAC targeting to the VDR target promoters appears not to require specific histone tail modifications by the co-regulators (Fig. 3). Thus, it is likely that WINAC associating on promoters escort VDR for its

Fig. 2. Ligand-dependent promoter targeting of co-regulators through WINAC-VDR association. (A) VDR-specific facilitation of co-activator accessibility by WINAC. MCF7 cells were transfected with the expression vectors of a luciferase reporter plasmid containing the GAL4 upstream activation sequence (UAS) [17mer(x2)] driven by the b-globin promoter (0.5 μg). PML-CMV (2 ng), GAL4-DBD-VDR-DEF (0.2 μg), GAL4-DBD-Era-DEF (0.2 μg), pDNA3-FLAG-WSTF (+: 0.1 μg; ++: 0.3 μg), pSV-Brg1 (0.2 μg), pSV-hBrm (0.2 μg), pcDNA3-TRAP220 (0.3 μg), pcDNA3-TIF2 (0.3 μg), siRNA (+: 0.1 μg; ++: 0.2 μg) of WSTF-RNAi, or control RNAi or their combinations were transfected as indicated in the panels in the absence or presence of ligand (10⁻⁹ M). Bars in each graph show the fold change in luciferase activity relative to the activity of the receptor transactivation in the presence of ligand. (B) ChIP analysis on the 24(OH)ase promoter and 1α(OH)ase promoter of WSTF stable transformants. Soluble chromatin was prepared from WSTF stable transformants treated with D3 (10⁻⁹ M) for 45 min and immunoprecipitated with indicated antibodies. (C and D) The co-regulator-like actions of WSTF on the naturally occurring positive and negative Vitamin D response elements. MCF7 cells were transfected with the expression vectors of either the luciferase reporter plasmid containing a human 24(OH)ase promoter harboring a canonical positive VDRE or a human 1α(OH)ase promoter containing a negative VDRE and the factors shown in (A) or together with pcDNA3-N-CoR (0.3 μg), pcDNA3-HDAC2 (0.3 μg). (E) WSTF-mediated regulations of endogenous genes by VDR. RT-PCR analysis of MCF7 cells was performed 12 h after the induction by D3 (10⁻⁹ M) [5].

recognition and specific binding to VDREs, through nucleosomal mobilization by WINAC, presumably co-operating with the other chromatin complexes [19]. Alternatively, once VDR happens to bind VDREs during non-specific chromatin remodeling, WINAC might be acquired to VDR upon the promoters to engage in local nucleosome reorganization [14].

## Acknowledgements

## References

[1] D.J. Mangelsdorf, C. Thummel, M. Beato, P. Herrlich, G. Schutz, K. Umesono, B. Blumberg, P. Kastner, M. Mark, P. Chambon, et al., The nuclear receptor superfamily: the second decade, Cell 83 (1995) 835–839.

[2] G.J. Narlikar, H.Y. Fan, R.E. Kingston, Cooperation between complexes that regulate chromatin structure and transcription, Cell 108 (2002) 475–487.

[3] B.M. Emerson, Specificity of gene regulation, Cell 109 (2002) 267–270.

[4] A.H. Hassan, P. Prochasson, K.E. Neely, S.C. Galasinski, M. Chandy, M.J. Carrozza, J.L. Workman, Function and selectivity of bromodomains in anchoring chromatin-modifying complexes to promoter nucleosomes, Cell 111 (2002) 369–379.

[5] J. Yanagisawa, H. Kitagawa, M. Yanagida, O. Wada, S. Ogawa, M. Nakagomi, H. Oishi, Y. Yamamoto, H. Nagasawa, S.B. McMahon, M.D. Cole, L. Tola, N. Takahashi, S. Kato, Nuclear receptor function requires a TFTC-type histone acetyl transferase complex, Mol. Cell. 9 (2002) 553–562.

[6] C. Rachez, D. Lemon, Z. Suldan, V. Bromleigh, M. Gamble, M. Naar, H. Erdjument, P. Tempst, P. Freedman, Ligand-dependent transcription activation by nuclear receptors requires the DRIP complex, Nature 398 (1999) 824–828.

[7] C.E. Brown, L. Howe, K. Sousa, S.C. Alley, M.J. Carrozza, S. Tan, J.L. Workman, Recruitment of HAT complexes by direct activator interactions with the ATM-related Tra1 subunit, Science 292 (2001) 2333–2337.

[8] D.V. Fyodorov, J.T. Kadonaga, The many faces of chromatin remodeling: SWItching beyond transcription, Cell 106 (2001) 523–525.

[9] D. Yasui, M. Miyano, S. Cai, P. Varga-Weisz, T. Kohwi-Shigematsu, SATB1 targets chromatin remodelling to regulate genes over long distances, Nature 419 (2002) 641–645.

[10] X. Lu, X. Meng, C.A. Morris, M.T. Keating, A novel human gene, WSTF, is deleted in Williams syndrome, Genomics 54 (1998) 241–249.

[11] M.H. Jones, N. Hamana, J. Nezu, M. Shimane, A novel family of bromodomain genes, Genomics 63 (2000) 40–45.

[12] R.J. Peoples, M.J. Cisco, P. Kaplan, U. Francke, Identification of the WBSCR9 gene, encoding a novel transcriptional regulator, in the Williams–Beuren syndrome deletion at 7q11.23, Cytogenet. Cell Genet. 82 (1998) 238–246.

[13] R.A. Poot, G. Dellaire, B.B. Hulsmann, M.A. Grimaldi, D.F. Corona, P.B. Becker, W.A. Bickmore, P.D. Varga-Weisz, HuCHRAC, a human ISWI chromatin remodelling complex contains hACF1 and two novel histone-fold proteins, EMBO J. 19 (2000) 3377–3387.

[14] H. Kitagawa, R. Fujiki, K. Yoshimura, Y. Mezaki, Y. Uematsu, D. Matsui, S. Ogawa, K. Unno, M. Okubo, A. Tokita, T. Nakagawa, T. Ito, Y. Ishimi, H. Nagasawa, T. Matsumoto, J. Yanagisawa, S. Kato, The chromatin remodeling complex WINAC targets a nuclear receptor to promoters and is impaired in Williams syndrome, Cell 113 (2003) 1–13.

[15] S. Smith, B. Stillman, Purification and characterization of CAF-I, a human cell factor required for chromatin assembly during DNA replication in vitro, Cell 58 (1989) 15–25.

[16] P.D. Varga-Weisz, M. Wilm, E. Bonte, K. Dumas, M. Mann, P.B. Becker, Chromatin-remodelling factor CHRAC contains the ATPases ISWI and topoisomerase II, Nature 388 (1997) 598–602.

[17] G. LeRoy, G. Orphanides, W.S. Lane, D. Reinberg, Requirement of RSF and FACT for transcription of chromatin templates in vitro, Science 282 (1998) 1900–1904.

[18] T. Ito, M. Bulger, M.J. Pazin, R. Kobayashi, J.T. Kadonaga, ACF, an ISWI-containing and ATP-utilizing chromatin assembly and remodeling factor, Cell 90 (1997) 145–155.

[19] B. Lemon, C. Inouye, D.S. King, R. Tjian, Selectivity of chromatin-remodelling cofactors for ligand-activated transcription, Nature 414 (2001) 924–928.

[20] Y. Shang, X. Hu, J. DiRenzo, M.A. Lazar, M. Brown, Cofactor dynamics and sufficiency in estrogen receptor-regulated transcription, Cell 103 (2000) 843–852.

[21] B. Belandia, R.L. Orford, H.C. Hurst, M.G. Parker, Targeting of SWI/SNF chromatin remodelling complexes to estrogen-responsive genes, EMBO J. 21 (2002) 4094–4103.

[22] A. Murayama, K. Takeyama, S. Kitanaka, Y. Kodera, T. Hosoya, S. Kato, The promoter of the human 25-hydroxyvitamin D3 1 alpha-hydroxylase gene confers positive and negative responsiveness to PTH, calcitonin, and 1 alpha, 25(OH)2D3, Biochem. Biophys. Res. Commun. 249 (1998) 11–16.

# Disruption of Nuclear Vitamin D Receptor Gene Causes Enhanced Thrombogenicity in Mice*

Ken-ichi Aihara‡§, Hiroyuki Azuma‡, Masashi Akaike‡, Yasumasa Ikeda‡, Michiko Yamashita¶, Toshiki Sudo‖, Hideki Hayashi‖, Yoshihisa Yamada‖, Fuminari Endoh**, Mitsunori Fujimura‡, Tomonori Yoshida‡, Hiroshi Yamaguchi‡, Shunji Hashizume‡, Midori Kato‡, Kimihiro Yoshimura‡‡, Yoko Yamamoto‡‡, Shigeaki Kato‡‡, and Toshio Matsumoto‡

From the ‡Department of Medicine and Bioregulatory Sciences and the ¶Department of Pathology, University of Tokushima Graduate School of Medicine, 3-18-15 Kuramoto-cho, Tokushima 770-8503, the ‖First Institute of New Drug Discovery, Otsuka Pharmaceutical Co. Ltd., 463-10 Kagasuno, Kawauchi-cho, Tokushima 771-0192, the **Anatomic and Molecular Division, TSL, Inc., Higashimatuyama Laboratory, 656-1 Higashidaira Higashimatsuyama-shi, Saitama 355-0002, and the ‡‡Institute of Molecular and Cellular Biosciences, the University of Tokyo, 1-1-1 Yayoi, Bunkyo-ku, Tokyo 113-0032, Japan

Vitamin D metabolites influence the expression of various genes involved in calcium homeostasis, cell differentiation, and regulation of the immune system. Expression of these genes is mediated by the activation of the nuclear vitamin D receptor (VDR). Previous studies have shown that a hormonally active form of vitamin D, 1α,25-dihydroxyvitamin D3, exerts anticoagulant effects in cultured monocytic cells. To clarify whether activation of VDR plays any antithrombotic actions *in vivo*, hemostatic/thrombogenic systems were examined in normocalcemic VDR knock-out (KO) mice on a high calcium diet and compared with wild type and hypocalcemic VDRKO mice that were fed a regular diet. Platelet aggregation was enhanced significantly in normocalcemic VDRKO mice compared with wild type and hypocalcemic VDRKO mice. Aortic endothelial nitric-oxide (NO) synthase expression and urinary NOx excretions were reduced in hypocalcemic VDRKO mice, but not in normocalcemic VDRKO mice. Northern blot and RT-PCR analyses revealed that the gene expression of antithrombin in the liver as well as that of thrombomodulin in the aorta, liver and kidney was down-regulated in hypo- and normocalcemic VDRKO mice. Whereas tissue factor mRNA expression in the liver and kidney was up-regulated in VDRKO mice regardless of plasma calcium level. Furthermore, VDRKO mice manifested an exacerbated multi-organ thrombus formation after exogenous lipopolysaccharide injection regardless of the calcemic conditions. These results demonstrate that activation of nuclear VDR elicits antithrombotic effects *in vivo*, and suggest that the VDR system may play a physiological role in the maintenance of antithrombotic homeostasis.

In many target organs, vitamin D exerts a variety of biological functions such as calcium homeostasis, cell proliferation, and cell differentiation. Most of these actions are exerted through the transcriptional control of target genes by the activation of the nuclear vitamin D receptor (VDR).[1] VDR is a ligand-inducible transcription factor that belongs to the nuclear receptor superfamily (1). VDR forms a heterodimer with the retinoid X receptor and binds to specific vitamin D-responsive elements on target genes (2, 3), which initiate sequences of events that lead to the activation or repression of target gene transcription by recruiting transcriptional cofactor complexes. Previous studies demonstrated that VDR knock-out (KO) mice manifest a variety of phenotypic abnormalities, including hypocalcemia, osteopenia, growth retardation, alopecia (4, 5), impaired immunity (6), hypertension with cardiac hypertrophy (7), and abnormal skeletal muscle development (8) and that most, but not all, of these phenotypic abnormalities can be rescued by normalization of serum mineral levels (6, 9).

In addition to its classical target tissues, VDR is also expressed in monocytic cells (10) and vascular endothelial cells (11), suggesting potential roles of vitamin D in antithrombotic functions. Koyama and colleagues (10, 12) have found that a hormonally active form of vitamin D, 1α,25-dihydroxyvitamin D3, as well as retinoic acid, exert anticoagulant effects by up-regulating the expression of the anticoagulant glycoprotein, thrombomodulin (TM), and by down-regulating the expression of a critical coagulation factor, tissue factor (TF), in cultured monocytic cells and human peripheral monocytes. However, it remains unclear whether activation of nuclear VDR can elicit antithrombotic actions *in vivo*. The present study was undertaken to clarify the physiological role of VDR-mediated actions in the hemostatic/thrombogenic system *in vivo*.

## EXPERIMENTAL PROCEDURES

*Animal Preparation*—VDR homozygous mutants (4) and wild type (WT) control littermates were maintained as hybrids with C57BL/6J and CBA genetic backgrounds in a specific pathogen-free facility with a 12-h light and dark cycle. As reported previously (4, 9), a lactose-rich high calcium diet can normalize hypocalcemia in VDRKO mice, whereas a high calcium diet causes considerable hypercalcemia in WT mice. Therefore, after weaning (at 3 weeks of age) we divided the mice into three groups as follows: group 1 are WT mice fed a regular diet (containing 1.2% calcium and 1.0% phosphorus, Japan Clea, Tokyo, Japan); group 2 are VDRKO mice fed a regular diet (hypocalcemic); and

---

[1] The abbreviations used are: VDR, vitamin D receptor; AT, antithrombin; eNOS, endothelial nitric-oxide synthase; GFD, glomeruli with fibrin deposition; KO, knock-out; LPS, lipopolysaccharide; NO, nitric oxide; NOx, NO metabolites; PTH, parathyroid hormone; RARE, retinoic acid-responsive element; RT, reverse transcription; TF, tissue factor; TM, thrombomodulin; VDRE, vitamin D-responsive element; VDRKO, vitamin D receptor knock-out; WT, wild type.

group 3 are VDRKO mice fed a lactose-rich high calcium diet (normo-calcemic). Experiments were conducted in 12-week-old mice that had been weaned then fed a specified diet for 9 weeks.

*Blood Collection*—Blood was collected from the inferior vena cava of mice under ether anesthesia. The blood was drawn with 21-gauge needles into plastic syringes containing 0.1 volume of 3.8% trisodium citrate solution. Some whole blood samples were used immediately for platelet aggregation analysis, and other whole blood samples were centrifuged at 2,000 × $g$ for 10 min to obtain plasma. The plasma was stored at −80 °C until assayed.

*Measurement of Plasma Calcium and Parathyroid (PTH) Hormone*—Plasma levels of calcium and PTH were determined using the OCPC method and a rat PTH IRMA Kit (Immunotopics, Inc., San Clemente, CA), respectively.

*Comparison of Platelet Aggregation with a Screen Filtration Pressure Method*—Measurements of platelet aggregation with a screen filtration pressure aggregometer (WBA analyzer from SSR Engineering Co., Ltd., Yokohama, Japan) were performed according to a method described previously (13, 14). Reaction tubes containing 200-$\mu$l aliquots of whole blood were placed in an incubation chamber at 37 °C for 30 s followed by the addition of 22.2 $\mu$l of a serial concentration (1, 2, 4, 8 or 16 $\mu$M) of ADP (Sigma). 2 min after the addition of ADP, the blood samples were filtered through microsieve screens connected to a pressure sensor. A negative pressure of −130 mm Hg was established as 100%. The 0% pressure base line was established as −6 mm Hg, rather than 0 mm Hg because of the viscosity of whole blood. The platelet aggregation pressure of each reaction tube was determined as the pressure rate (percent). For the screen filtration pressure aggregometer study, the pressure rate was standardized using a grading curve produced by plotting four or five concentrations of ADP on the $x$ axis and pressure rate (percent) on the $y$ axis. The concentration of ADP causing a 50% increase in pressure rate was calculated and applied as the platelet aggregatory threshold index.

*Measurement of Daily Urinary Excretion of Nitric Oxide Metabolites*—To evaluate urinary excretion of nitric oxide (NO) metabolites (NOx), mice were housed individually in metabolic cages that provided free access to tap water and food for 24 h. NOx levels, from the murine urine, were determined by high performance liquid chromatography (15).

*Estimation of Plasma Prothrombin Time and Activated Partial Thromboplastin Time*—Plasma prothrombin time and activated partial thromboplastin time were determined by a scattered light detection method (16).

*Measurement of Plasma Antithrombin (AT) Activity*—Plasma AT activity was measured using N-test ATIII-S (Nittobo, Tokyo, Japan), which determines anticoagulant activity using a chromogenic substrate, according to the manufacturer's instructions.

*Western Blot Analysis*—Aortic tissue samples were homogenized in an ice-cold tissue protein extraction reagent (T-PER™, Pierce) containing protease inhibitors. Equal amounts of protein (50 $\mu$g) were loaded onto 10% acrylamide gels and then transferred to nitrocellulose membranes using a wet blot apparatus. Membranes were blocked overnight at 4 °C in blocking buffer (10 mM Tris-HCl, 10 mM NaCl, 0.1% polyoxyethylenesorbitan monolaurate) with 5% skim milk. The first antibody, mouse anti-human endothelial nitric-oxide synthase (eNOS) monoclonal antibody (1:1000 dilution, BD Transduction Laboratories, San Jose, CA), was applied for 1 h at room temperature. After a 30-min wash with the blocking buffer, membranes were probed with the second antibody (1:5000 dilution anti-mouse IgG horseradish peroxidase-linked whole antibody, Amersham Biosciences) for 1 h at room temperature. Membranes were washed again for 30 min. The membranes were then incubated with chemiluminescent reagents (ECL Western blotting Detection Reagents, Amersham Biosciences) for 5 min and then exposed to x-ray film. Band intensities were quantified using a NIH Image system.

*RNA Isolation*—Aortas, livers, and kidneys were rinsed with physiological saline. Total RNA was isolated by an acid guanidinium thiocyanate-phenol-chloroform extraction using TRIzol Reagent (Invitrogen). RNA concentrations were measured spectrophotometrically at 260 nm, and then samples were stored in diethyl dicarbonate-treated water at −80 °C.

*Northern Blot Analysis*—Approximately 20 $\mu$g of total RNA of the liver was fractionated on 1% formaldehyde-agarose gels and transferred to Hybond nylon membranes (Amersham Biosciences) by capillary action in a high salt solution (20 × SSC). Blots were prehybridized in a hybridization solution for 1 h at 42 °C followed by overnight hybridization with a digoxigenin-labeled specific oligonucleotide probe (DIG Northern Starter Kit, Roche Applied Science). Blots were washed

twice in 2 × SSC and 0.1% SDS at room temperature for 5 min and then washed twice in 0.2 × SSC and 0.1% SDS at 68 °C for 15 min before exposure to x-ray film. The forward and reverse sequences of the AT oligonucleotide probe were: 5'-ATGATGTACCAGGAAGGCAA-3' and 5'-GGAATGCGTCGGAGACATAG-3', respectively. AT mRNA was estimated after correcting for loading differences by measuring the amount of 28 S rRNA.

*RT-PCR Analysis*—Expression of TF, TM, and glucose-3-phosphate dehydrogenase mRNA in aorta, liver, and kidney tissue were quantified by a RT-PCR method (8). Primers used were as follows: TF, forward 5'-CGGGTGCAGGCATTCCAGAG-3' and reverse 5'-CTCCGTGGGAC-AGAGAGGAC-3'; TM, forward 5'-CAGGCTACCAGTTGGCTGCAG-3' and reverse 5'-AGAGTTAGGGTCACAGTCTGC-3'; glucose-3-phosphate dehydrogenase; forward 5'-ACCACAGTCCATGCCATCA-C-3' and reverse 5'-TCCACCACCCTGTTGCTGTA-3'. PCR products were electrophoresed on 2.0% agarose gels, stained with ethidium bromide, visualized by ultraviolet transillumination, and photographed. Expression levels of TF and TM were expressed relative to the glucose-3-phosphate dehydrogenase signal.

*Lipopolysaccharide-induced Thrombus Formation Experiments and Immunohistochemical Analysis*—Mice were injected intraperitoneally with 5 mg/kg lipopolysaccharide (LPS) (*Escherichia coli* serotype 0111: B4; Sigma). 6 h later, mice were sacrificed, and lung, aorta, liver, and kidney tissue were removed. The tissue samples were placed immediately in 20% neutrally buffered formalin and stored overnight. After fixation, samples were embedded in paraffin, and 3-$\mu$m thick sections were produced. These tissue sections were deparaffinized, hydrated, and treated with a protease mixture (P-8038, Sigma) for 10 min at room temperature. After washing with deionized water, endogenous peroxidase was blocked with 3% hydrogen peroxide for 5 min, and then endogenous biotin was blocked with the DAKO Biotin Blocking System (DAKO Cytometion, Glostrup, Denmark). After washing with deionized water and blocking nonspecific staining by incubation with 10% porcine serum (GEMINI Bio-Products, Woodland, CA) in phosphate-buffered saline for 10 min at room temperature, the slides were incubated with rabbit anti-human fibrin-fibrinogen antibody (DAKO, 1:200 dilution) overnight at 4 °C. The slides were then rinsed with phosphate-buffered saline and incubated with (1:500) biotinylated F(ab')$_2$ fragments of swine anti-rabbit immunoglobulins (DAKO) for 30 min at room temperature. After rinsing with phosphate-buffered saline, the slides were incubated with diluted (1:500) peroxidase-conjugated streptavidin (DAKO) for 30 min at room temperature. Following incubation in 100 ml of phosphate-buffered saline containing 20 mg of 3,3'-diaminobenzidine tetrahydrochloride, 20 $\mu$l of 30% hydrogen peroxide, and 65 mg of sodium azide for 5 min at room temperature, the slides were counterstained with hematoxylin for 1 min. Finally, the sections were mounted after washing with deionized water and dehydration. The percentage of the glomeruli with fibrin deposition (% GFD) were calculated in all areas of each histological specimen of the kidney. Partially stained glomeruli were categorized as positive.

*Statistical Analysis*—Values for each parameter within a group were expressed as the mean ± S.E. For comparisons between genotypes, statistical significance was assessed using a one-way analysis of variance. Statistical significance was considered at $p < 0.05$.

## RESULTS

*Plasma Calcium and PTH Levels in WT and VDRKO Mice*—The plasma calcium levels of VDRKO mice fed a regular diet were significantly low compared with WT mice (Fig. 1A). When VDRKO mice were fed a high calcium diet, plasma calcium levels were restored to levels similar to those in WT mice (Fig. 1A). As expected, marked elevation in plasma PTH levels were detected in VDRKO mice compared with WT mice. Consistent with the normalization of hypocalcemia from a high calcium diet (Fig. 1B), elevated plasma PTH levels decreased to similar levels observed in WT mice.

*Aberrant Platelet Aggregation in VDRKO Mice*—To examine the effect of VDR activation on platelet function, we first evaluated ADP-induced whole blood aggregation using a screen filtration pressure method in 12-week-old mice (Fig. 2A). Platelet aggregatory threshold index values in hypocalcemic VDRKO mice were increased markedly compared with those in WT mice ($p < 0.01$) (Fig. 2B). In contrast, platelet aggregatory threshold index values in normocalcemic VDRKO mice were significantly lower than those in WT mice ($p < 0.05$) (Fig. 2B).
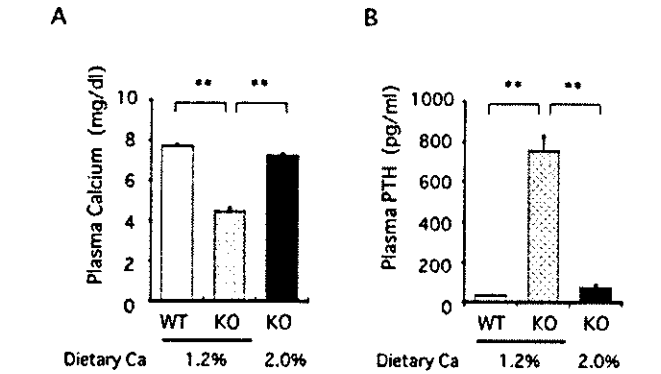
A           B



FIG. 1. Plasma levels of calcium (A) and PTH (B) in WT mice and VDRKO mice at 12 weeks of age. The number of mice examined in A and B was: 18 (WT, 1.2% calcium), 14 (KO, 1.2% calcium), and 14 (KO, 2.0% calcium). Values are expressed as the mean ± S.E. **, $p <$ 0.01.
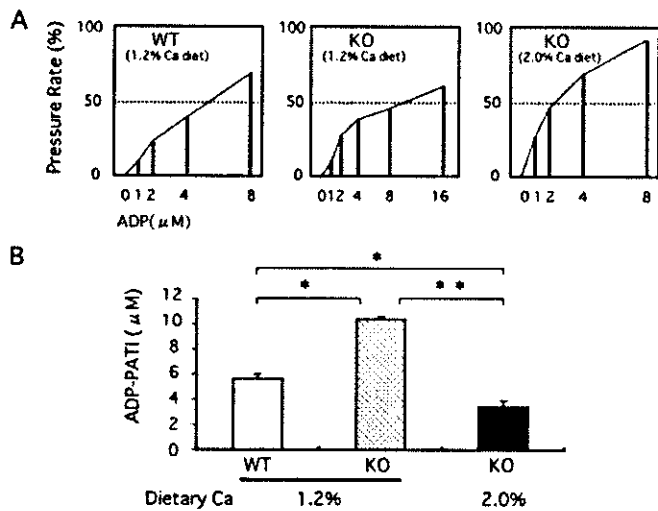
A



B



FIG. 2. Representative results of platelet aggregation analyzed by the screen filtration pressure method in WT mice (1.2% calcium) and VDRKO mice (1.2% calcium, 2.0% calcium) at 12 weeks of age. A, four or five different concentrations of agonist (ADP) were plotted along the horizontal axis, and their individual pressure rates (percent) were plotted along the vertical axis. B, the mean concentrations of agonist inducing a 50% pressure rate were calculated as the platelet aggregatory threshold index (PATI). The number of mice examined was: 14 (WT, 1.2% calcium), 10 (KO, 1.2% calcium), and 14 (KO, 2.0% calcium). Values are expressed as the mean ± S.E. *, $p <$ 0.05, **, $p <$ 0.01.

These results demonstrate that hypocalcemia is responsible for the suppression of platelet aggregation in VDRKO mice fed a regular diet and that VDR itself has a suppressive effect on platelet aggregability.

*Decreased Urinary Level of Nitric Oxide Metabolites in Hypocalcemic VDRKO Mice Was Restored by a High Calcium Diet*—Because platelet aggregation is affected by the bioavailability of NO, we then analyzed urinary excretion of NOx (Fig. 3A). Daily urinary excretion of NOx in VDRKO mice was decreased significantly compared with WT mice. Feeding a high calcium diet (2.0% calcium) restored the urinary level of NOx in VDRKO mice to a level similar to that in WT mice. Thus, it is unlikely that the enhanced platelet aggregation in normocalcemic VDRKO mice is mediated by a change in NO level.

*Impaired Aortic eNOS Expression in Hypocalcemic VDRKO Mice Was Normalized by High Calcium Diet*—Western blot analysis demonstrated that eNOS protein levels in hypocalcemic VDRKO mice decreased to 45 ± 20% of WT mice. This may be a cause of decreased levels of urinary NOx excretion in hypocalcemic VDRKO mice (Fig. 3B). By feeding a high calcium

A           B

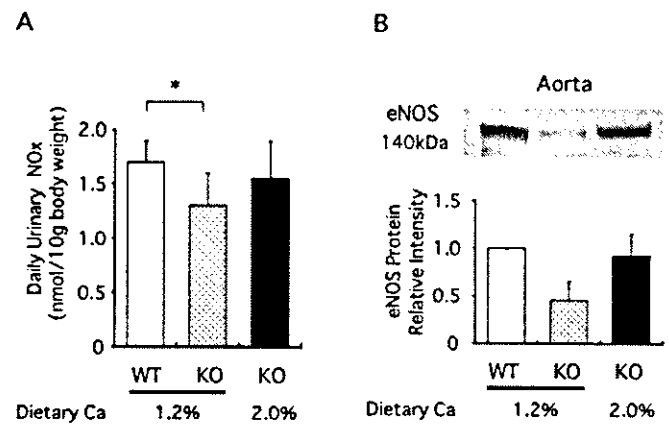

FIG. 3. A, daily urinary excretion levels of NOx in WT mice (1.2% calcium) and VDRKO mice (1.2% calcium, 2.0% calcium) at 12 weeks of age. The number of mice examined was: 18 (WT, 1.2% calcium), 14 (KO, 1.2% calcium), and 14 (KO, 2.0% calcium). Values are expressed as the mean ± S.E. *, $p <$ 0.05. B, Western blot analysis of eNOS protein levels in the aorta. Protein levels of eNOS in aortic tissues of WT mice (1.2% calcium) and VDRKO mice (1.2% calcium, 2.0% calcium) at 12 weeks of age were determined by Western blot analysis and quantified densitometrically. Each lane contains 50 μg of protein. Six aortic tissues were examined in each group.
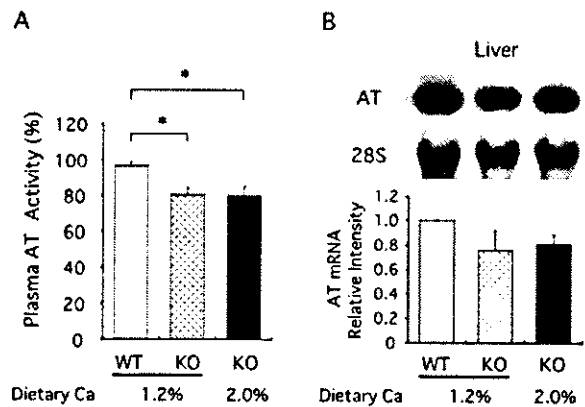
A           B



FIG. 4. A, plasma AT activity in WT mice (1.2% calcium) and VDRKO mice (1.2% calcium, 2.0% calcium) at 12 weeks of age. The number of mice examined was: 18 (WT, 1.2% calcium), 18 (KO, 1.2% calcium), and 16 (KO, 2.0% calcium). Values are expressed as the mean ± S.E. *, $p <$ 0.05. B, Northern blot analysis of hepatic AT gene expression in WT mice (1.2% calcium) and VDRKO mice (1.2% calcium, 2.0% calcium) at 12 weeks of age. Six individual hepatic tissue samples were examined in each group. Values are expressed as the mean ± S.E.

diet, eNOS protein levels in VDRKO mice returned to levels similar to those in WT mice (Fig. 3B). These results indicate that reduced eNOS protein levels in VDRKO mice are mediated by hypocalcemia.

*VDRKO Mice Manifested Normal Prothrombin Time and Activated Partial Thromboplastin Time*—Although prothrombin time and activated partial thromboplastin time in WT, hypo-, and normocalcemic VDRKO mice were measured, no significant differences were noted among these mice in either prothrombin time (10.6 ± 0.4, 10.6 ± 0.2, 10.8 ± 0.6 s in WT, hypo-, and normocalcemic VDRKO mice, respectively) or activated partial thromboplastin time (58.0 ± 3.8, 54.5 ± 4.4, 56.4 ± 6.0 s in WT, hypo-, and normocalcemic VDRKO mice, respectively). These results demonstrate that the loss of VDR function does not lead to impaired blood coagulation and is consistent with the fact that VDRKO mice do not show a bleeding tendency.

*Reduced Plasma Activity and Gene Expression of Antithrombin in VDRKO Mice*—We next examined the plasma activity of
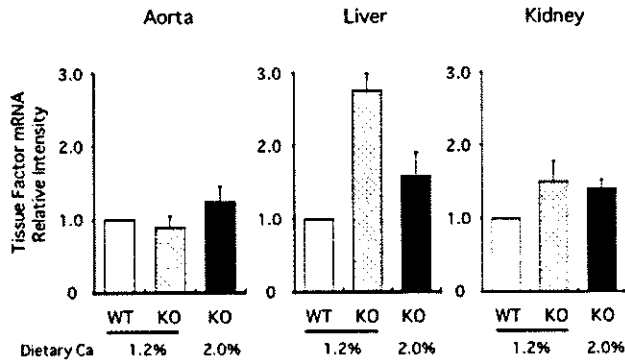
Aorta    Liver    Kidney



FIG. 5. **Quantitative analysis of TF mRNA levels in the aorta, liver, and kidney were performed by RT-PCR as described under "Experimental Procedures."** Total RNA was isolated from each organ of WT mice (1.2% calcium) and VDRKO mice (1.2% calcium, 2.0% calcium) at 12 weeks of age. Six individual tissue samples were examined in each group. Values are expressed as the mean ± S.E.
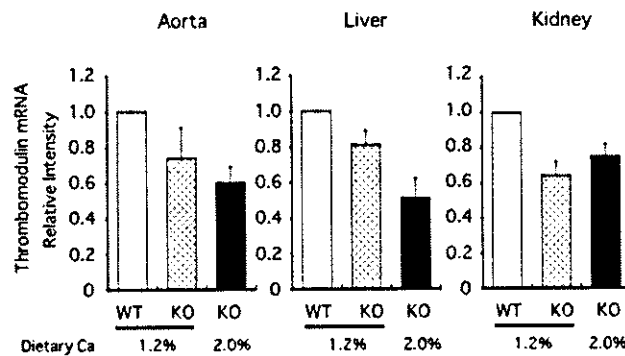
Aorta    Liver    Kidney



FIG. 6. **TM mRNA levels in the aorta, liver, and kidney were analyzed by RT-PCR as described under "Experimental Procedures."** Total RNA was isolated from each organ of WT mice (1.2% calcium) and VDRKO mice (1.2% calcium, 2.0% calcium) at 12 weeks of age. Six individual aorta, liver, and kidney tissue samples were examined in each group. Values are expressed as the mean ± S.E.

AT in these mice. Mean activities of plasma AT showed reductions in VDRKO mice regardless of their plasma calcium levels compared with those in WT mice (Fig. 4A). In addition, gene expression levels of AT in the liver were reduced by ~20% in both hypo- and normocalcemic VDRKO mice compared with those in WT mice (Fig. 4B). These results demonstrate that activated VDR positively regulates AT gene expression in the liver.

*Aberrant Gene Expression of TF and TM in VDRKO Mice*—As shown in Fig. 5, TF mRNA expression levels in the liver and kidney were enhanced in both hypo- and normocalcemic VDRKO mice compared with those in WT mice and tended to be higher in the aorta of normocalcemic VDRKO mice. In contrast, TM mRNA levels in the aorta, liver, and kidney were all reduced in VDRKO mice compared with those in WT mice (Fig. 6). Normalization of plasma calcium levels failed to correct the aberrant expression patterns of TF and TM genes in VDRKO mice (Figs. 5 and 6). These results indicate that activation of VDR elicits down-regulation of TF and up-regulation of TM gene expression, *in vivo*.

*LPS-induced Thrombus Formation Was Exacerbated in VDRKO Mice*—To test the possibility that the VDR system counteracts thrombotic stimuli, 5 mg/kg LPS was injected intraperitoneally to WT and VDRKO mice. All mice survived the treatment until sacrifice. Immunohistochemical analysis revealed that hypo- and normocalcemic VDRKO mice exhibited increased fibrin deposition in the glomeruli and peritubular capillaries of the kidney compared with WT mice (Fig. 7). Exacerbated fibrin deposition was also noted in the hepatic
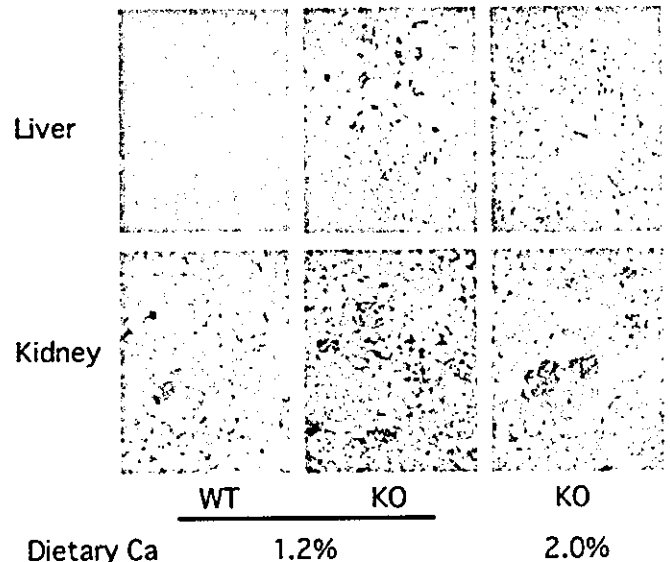


FIG. 7.**Immunohistochemical stainings with anti-fibrin-fibrinogen antibody of the liver** (*upper panels*) **and kidney** (*lower panels*) **after LPS injection, in WT mice (1.2% calcium) and VDRKO mice (1.2% calcium, 2.0% calcium) at 12 weeks of age.** Larger numbers of fibrin depositions were detected in both VDRKO mice compared with WT mice. Magnification, ×200.
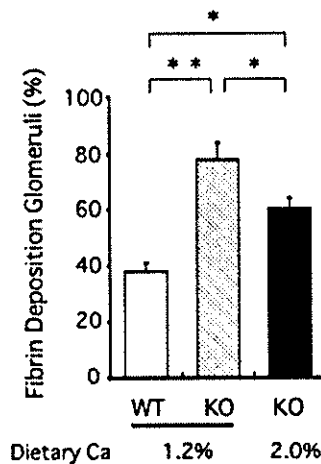


FIG. 8. **Percentage of glomeruli with fibrin deposition after LPS injection in WT mice (1.2% calcium) and VDRKO mice (1.2% calcium, 2.0% calcium) at 12 weeks of age.** LPS was injected intraperitoneally into mice as described under "Experimental Procedures." After 6 h, renal specimens were subjected to immunohistochemical analysis. The percentage of glomeruli with fibrin deposition was significantly higher in VDRKO mice than WT mice. Six individual renal tissue samples were examined in each group. Values are expressed as the mean ± S.E. *, $p < 0.05$, **, $p < 0.01$.

sinusoids of VDRKO mice regardless of plasma calcium levels (Fig. 7). No fibrin deposition was observed in the aorta or lung tissues from any group of mice (data not shown). To compare the degree of fibrin deposition quantitatively in the kidney, we compared the % GFD among three groups of mice. As shown in Fig. 8, the % GFD was significantly higher in both hypo- and normocalcemic VDRKO mice than that in WT mice. No fibrin deposition in the liver and kidney was observed when a vehicle was injected in both types of VDRKO mice (data not shown).

DISCUSSION

The present study demonstrates that ADP-induced platelet aggregation was enhanced significantly in normocalcemic VDRKO mice. Platelets are fragments of megakaryocytes that contribute to thrombus formation (17). Both normal hemostasis

and abnormal thrombosis depend on various regulatory factors within platelets (18). Physiological plasma calcium concentration is among the most important factors for normal platelet aggregation. Coordination of calcium flux through platelet-platelet contact serves to propagate calcium signaling throughout the developing thrombus to maintain thrombus growth (19). Thus, it is plausible to assume that the impaired platelet aggregation in hypocalcemic VDRKO mice was caused by the hypocalcemia in these mice. In contrast, molecular mechanisms underlying the accelerated platelet aggregation in normocalcemic VDRKO mice are unknown, and further investigations are required to understand VDR function in megakaryocytes and platelets.

There have been *in vitro* studies demonstrating that a hormonally active form of vitamin D up-regulates TM gene expression and down-regulates TF gene expression in monocytic cells (10, 12). However, *in vivo* effects of the vitamin D/VDR system on these factors have never been tested. In the present study, the gene expression of AT in the liver as well as that of TM in the aorta, liver, and kidney in VDRKO mice was down-regulated, whereas TF mRNA expression in the liver and kidney was up-regulated in VDRKO mice regardless of plasma calcium levels. Thus, the vitamin D/VDR system is shown to enhance the expression of antithrombotic factors while inhibiting the expression of a thrombogenic factor, TF.

AT is a plasma glycoprotein synthesized by hepatocytes and is one of the crucial inhibitors of blood coagulation through thrombin inactivation. Recently, AT-deficient mice were generated by gene targeting, and homozygous AT-null mice were shown to be prenatally lethal because of extensive thrombosis in the myocardium and liver sinusoids along with generally massive bleeding (20). In addition, heterozygous AT-deficient mice showed a tendency toward thrombus formation in the kidney after LPS injection (21). The present observations suggest that the vitamin D/VDR system may affect AT activity through transcriptional control of AT gene expression. Although Niessen *et al.* (22) reported ligand-dependent enhancement of human AT gene expression by retinoid X receptor $\alpha$ and thyroid hormone receptor $\beta$, their study revealed no effect of 1$\alpha$,25-dihydroxyvitamin D3 on AT production. The reason why they were unable to observe the effect of the vitamin D/VDR system on AT gene transcription may be the use of a shortened AT gene promoter in their study (22).

Because all-*trans*-retinoic acid up-regulates TM expression in both monocytic and vascular endothelial cells via the retinoic acid-responsive element (RARE)-mediated transcriptional activation of the TM gene (10), and because RARE on the TM gene promoter is very similar to the vitamin D-responsive element (VDRE), there is a possibility that the effect of the vitamin D/VDR system on the up-regulation of TM gene expression is mediated via the binding of liganded VDR to the RARE of the TM gene (10, 12). In contrast, there is no evidence for transcriptional regulation of TF gene expression by the vitamin D/VDR system through VDRE or RARE. The TF gene promoter contains two activator protein-1 binding sites and a nuclear factor-$\kappa$B site, and functional interactions between these two factors are required for maximal induction of TF gene transcription by tumor necrosis factor-$\alpha$ in vascular endothelial cells and by LPS in monocytic cells (23). Because interleukin-12 production from activated monocytic THP-1 cells is suppressed by 1$\alpha$,25-dihydroxyvitamin D3 through the inhibition of nuclear factor-$\kappa$B activation (24), the vitamin D/VDR system may suppress TF gene expression via modulation of nuclear factor-$\kappa$B activation.

The present study also demonstrates that VDRKO mice manifest an exacerbated multiorgan thrombus after exogenous

LPS injection regardless of the calcemic conditions. In agreement with the present results, Asakura *et al.* (25) demonstrated a beneficial effect of the active form of vitamin D3 against thrombosis, using a LPS-induced disseminated intravascular coagulation rat model. Enhanced platelet aggregation, down-regulated expression of AT and TM along with up-regulation of TF expression in both hypo- and normocalcemic VDRKO mice can all contribute to the enhanced thrombogenicity of VDRKO mice. In addition, deficiency of NO is associated with arterial thrombosis and thrombus formation in the renal vasculature of animal models and patients with endothelial dysfunction (26, 27). However, because reduced eNOS levels and urinary NOx excretion in hypocalcemic VDRKO mice were reversed in normocalcemic VDRKO mice, the exacerbated thrombus formation caused by LPS injection in normocalcemic VDRKO mice cannot be explained by a change in NO production. Although further investigation is needed to clarify the antithrombogenic effects of vitamin D3, the present results are consistent with the notion that the vitamin D/VDR system plays an important role in maintaining normal antithrombotic homeostasis *in vivo*.

REFERENCES

1. Mangelsdorf, D. J., Thummel, C., Beato, M., Herrlich, P., Schutz, G., Umesono, K., Blumberg, B., Kastner, P., Mark, M., and Chambon, P. (1995) *Cell* **83**, 835–839
2. Haussler, M. R., Whitfield, G. K., Haussler, C. A., Hsieh, J. C., Thompson, P. D., Selznick, S. H., Dominguez, C. E., and Jurutka, P. W. (1998) *J. Bone Miner. Res.* **13**, 325–349
3. Takeyama, K., Masuhiro, Y., Fuse, H., Endoh, H., Murayama, A., Kitanaka, S., Suzawa, M., Yanagisawa, J., and Kato, S. (1999) *Mol. Cell. Biol.* **19**, 1049–1055
4. Yoshizawa, T., Handa, Y., Uematsu, Y., Takeda, S., Sekine, K., Yoshihara, Y., Kawakami, T., Arioka, K., Sato, H., Uchiyama, Y., Masushige, S., Fukamizu, A., Matsumoto, T., and Kato, S. (1997) *Nat. Genet.* **16**, 391–396
5. Li, Y. C., Pirro, A. E., Amling, M., Delling, G., Baron, R., Bronson, R., and Demay, M. B. (1997) *Proc. Natl. Acad. Sci. U. S. A.* **94**, 9831–9835
6. Mathieu, C., Van Etten, E., Gysemans, C., Decallonne, B., Kato, S., Laureys, J., Depovere, J., Valckx, D., Verstuyf, A., and Bouillon, R. (2001) *J. Bone Miner. Res.* **16**, 2057–2065
7. Li, Y. C., Kong, J., Wei, M., Chen, Z. F., Liu, S. Q., and Cao, L. P. (2002) *J. Clin. Invest.* **110**, 229–238
8. Endo, I., Inoue, D., Mitsui, T., Umaki, Y., Akaike, M., Yoshizawa, T., Kato, S., and Matsumoto, T. (2003) *Endocrinology* **144**, 5138–5144
9. Li, Y. C., Amling, M., Pirro, A. E., Priemel, M., Meuse, J., Baron, R., Delling, G., and Demay, M. B. (1998) *Endocrinology* **139**, 4391–4396
10. Koyama, T., Shibakura, M., Ohsawa, M., Kamiyama, R., and Hirosawa, S. (1998) *Blood* **92**, 160–167
11. Merke, J., Milde, P., Lewicka, S., Hugel, U., Klaus, G., Mangelsdorf, D. J., Haussler, M. R., Rauterberg, E. W., and Ritz, E. (1989) *J. Clin. Invest.* **83**, 1903–1915
12. Ohsawa, M., Koyama, T., Yamamoto, K., Hirosawa, S., Kamei, S., and Kamiyama, R. (2000) *Circulation* **102**, 2867–2872
13. Ozeki, Y., Sudo, T., Toga, K., Nagamura, Y., Ito, H., Ogawa, T., and Kimura, Y. (2001) *Thromb. Res.* **101**, 65–72
14. Sudo, T., Ito, H., and Kimura, Y. (2003) *Platelets* **14**, 239–246
15. Yamada, K., and Nabeshima, T. (1997) *J. Neurochem.* **68**, 1234–1243
16. Poller, L. (1988) *Thromb. Haemostasis* **60**, 18–20
17. Abrams, C., and Shattil, S. J. (1991) *Thromb. Haemostasis* **65**, 467–473
18. Nielsen, H. K. (1991) *Semin. Thromb. Hemostasis* **17**, (Suppl. 3) 250–253
19. Nesbitt, W. S., Giuliano, S., Kulkarni, S., Dopheide, S. M., Harper, I. S., and Jackson, S. P. (2003) *J. Cell Biol.* **160**, 1151–1161
20. Ishiguro, K., Kojima, T., Kadomatsu, K., Nakayama, Y., Takagi, A., Suzuki, M., Takeda, N., Ito, M., Yamamoto, K., Matsushita, T., Kusugami, K., Muramatsu, T., and Saito, H. (2000) *J. Clin. Invest.* **106**, 873–878
21. Yanada, M., Kojima, T., Ishiguro, K., Nakayama, Y., Yamamoto, K., Matsushita, T., Kadomatsu, K., Nishimura, M., Muramatsu, T., and Saito, H. (2002) *Blood* **99**, 2455–2458
22. Niessen, R. W., Rezaee, F., Reitsma, P. H., Peters, M., de Vijlder, J. J., and Sturk, A. (1996) *Biochem. J.* **318**, 263–270
23. Mackman, N. (1997) *Thromb. Haemostasis* **78**, 747–754
24. D'Ambrosio, D., Cippitelli, M., Cocciolo, M. G., Mazzeo, D., Di Lucia, P., Lang, R., Sinigaglia, F., and Panina-Bordignon, P. (1998) *J. Clin. Invest.* **101**, 252–262
25. Asakura, H., Aoshima, K., Suga, Y., Yamazaki, M., Morishita, E., Saito, M., Miyamoto, K., and Nakao, S. (2001) *Thromb. Haemostasis* **85**, 287–290
26. Loscalzo, J., Freedman, J., Inbal, A., Keaney, J. F., Jr., Michelson, A. D., and Vita, J. A. (2000) *Trans. Am. Clin. Climatol. Assoc.* **111**, 158–163
27. Verhagen, A. M., Rabelink, T. J., Braam, B., Opgenorth, T. J., Grone, H. J., Koomans, H. A., and Joles, J. A. (1998) *J. Am. Soc. Nephrol.* **9**, 755–762

# BRCA1 function mediates a TRAP/DRIP complex through direct interaction with TRAP220

Osamu Wada[1,2], Hajime Oishi[1,2], Ichiro Takada[1,3], Junn Yanagisawa[1,3], Tetsu Yano*[,1] and Shigeaki Kato[1,3]

[1]Institute of Molecular and Cellular Biosciences, University of Tokyo, Yayoi 1-1-1, Bunkyo-ku, Tokyo 113-0034, Japan; [2]Department of Obstetrics and Gynecology, University of Tokyo, Hongo 7-3-1, Bunkyo-ku, Tokyo 113-8655, Japan; [3]SORST, Japan Science and Technology, Honcho 4-1-8, Kawaguchi, Saitama 332-0012, Japan

Breast cancer susceptibility gene 1 (BRCA1) is a tumor suppressor gene mutated in a high percentage of hereditary breast and ovarian cancers. The multifunctional BRCA1 protein acts on cell cycle control, exerting several highly specialized DNA repair processes through diverse domains. Gene regulation through its C-terminal domain (BRCT) is indispensable for BRCA1-mediated tumor suppression, suggesting the possibility that the BRCT domain interacts with co-regulator complexes. Using a biochemical approach with HeLa S3 nuclear extracts, we isolated BRCT-associated complexes and identified one of the purified components as TRAP220. We then performed interaction studies in vivo (co-immunoprecipitation) and in vitro (glutathione S-transferase pull-down assays) and showed that BRCT directly interacted with TRAP220. This in vitro interaction was completely abolished by BRCT point mutations typical of those found in patients with BRCA1 that lack transactivation function. BRCA1 transactivation function was dependent on TRAP220 expression level in a transient expression assay. Moreover, a cell survival assay showed that antisense TRAP220 expression to disrupt endogenous TRAP220 expression significantly reduced the survival rate potentiated by BRCA1 after DNA damage. These results suggested that a TRAP220 complex play an important role as putative co-activator complexes in BRCA1-mediated tumor suppression.
Oncogene (2004) 23, 6000–6005. doi:10.1038/sj.onc.1207786
Published online 21 June 2004

Keywords: BRCA1; TRAP220; breast cancer

Germ-line mutation of BRCA1 is well known to predispose women to early onset of breast and ovarian cancer (Venkitaraman, 2002). The BRCA1 gene encodes a relatively large protein of 1863 amino acids, and apart from an N-terminal zinc-binding RING domain and two C-terminal tandem copies of a BRCT motif,

displays little similarity to other known proteins (Futreal et al., 1994; Miki et al., 1994). The C-terminal BRCT domain has been shown to be involved in double-stranded DNA repair and homologous recombination (Callebaut and Mornon, 1997; Moynahan et al., 1999; Scully et al., 1999; Zhong et al., 1999). However, the major function of BRCT is thought to be as a gene regulator, mediating BRCA1 function as a tumor suppressor. This hypothesis is based on several lines of evidence, including that the autonomous transactivation function of BRCA1 was preserved in a recombinant protein consisting of the BRCT domain fused to a GAL4 DNA-binding domain (Miyake et al., 2000). In addition, missense and point mutations in the BRCT domain derived from patients with inherited breast cancer result in the loss of transcriptional activity, and BRCA1 can also act as a negative regulator on some gene promoters (Chapman and Verma, 1996; Monteiro et al., 1996; Zheng et al., 2001; Kawai et al., 2002). Reflecting the complex nature of BRCT transactivation function, this domain has already been shown to physically interact with a number of transcription factors and co-regulators (presumably in complexes), and also associate with chromatin remodeling complexes (Anderson et al., 1998; Yu et al., 1998; Zhang et al., 1998; Yarden and Brody, 1999; Bochar et al., 2000). Moreover, transcriptional squelching between BRCA1 and estrogen receptor (ER) has recently been reported (Fan et al., 1999; Zheng et al., 2001). As ER is a member of the nuclear receptor (NR) gene superfamily and acts as a ligand-induced transcription factor (Mangelsdorf et al., 1995; Watanabe et al., 2001; Yanagisawa et al., 2002), limited cellular amounts of a common co-activator complex for both BRCA1 and ER could explain the transcriptional squelching phenomenon.

To better understand the BRCT transactivation function, we screened for putative transcription co-activator complexes that directly interacted with the BRCT domain using a biochemical approach. We established an affinity column whereby the BRCT domain (amino acids 1528–1863) was immobilized as a glutathione S-transferase (GST)-fusion protein. Fractions of HeLa S3 nuclear extract, presumably containing multiprotein complexes, were applied to the affinity
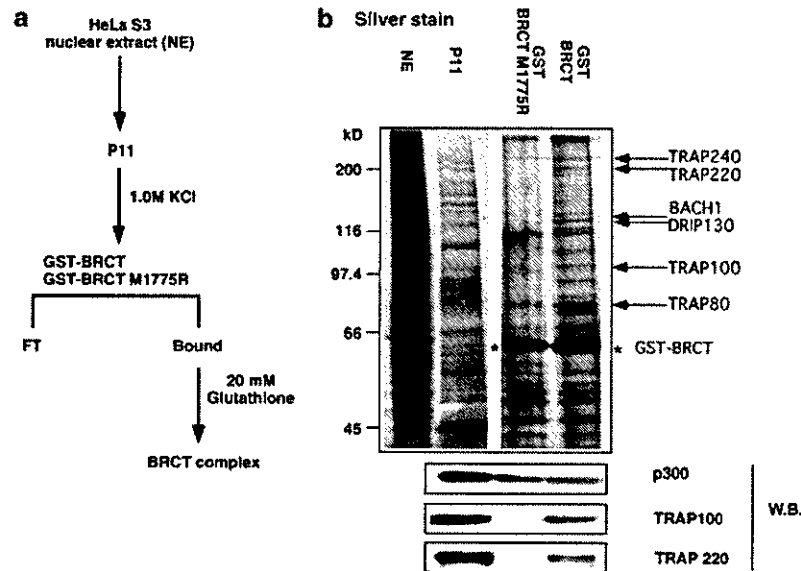
**Figure 1** Affinity purification of BRCT-containing complexes (a) Purification scheme. HeLa S3 nuclear extract was fractionated using a phosphocellulose (P11) column and a GST-BRCT (amino acids 1528–1863) affinity column. The 1 M KCl P11 eluate was concentrated onto the GST-BRCT affinity column at 4°C for 10–12 h. Bound proteins were washed extensively with buffer, and subsequently eluted by buffer containing 20 mM reduced glutathione. As a negative control, purification from P11 eluates was performed using another affinity column (immobilized GST-BRCT M1775R). (b) Purified fractions were boiled, separated by electrophoresis and analysed by SDS–PAGE followed by silver staining or Western blot analysis using antibody, as shown on the right of the figure. Molecular weight standards are shown to the left of the figure. The asterisk denotes the molecular bait (GST-BRCT, GST-BRCT M1775R) after elution. Arrows show proteins identified by mass spectrometry (Yanagisawa et al., 2002)

column (Yanagisawa et al., 2002; Kitagawa et al., 2003), and several of the transcription co-regulators subsequently verified in the BRCT-interacting complexes by Western blotting (Figure 1b, lower panel). Western blotting of the BRCT-interacting complexes identified TRAP220 and TRAP100 (Figure 1b), which were confirmed as factors that associate with BRCT by time-of-flight mass spectrometry (TOF-MS). TRAP220 contains two LXXLL motifs, which are consensus interacting motifs and part of the core activation domain in NR ligand-binding domains (Fondell et al., 1999; Rachez et al., 1999). Thus, TRAP220 is thought to act as a major and direct interactant with ER (Yanagisawa et al., 2002), as well as with other NRs, as part of the common TRAP/DRIP co-activator complex (Rachez et al., 1999). It is therefore possible that the functional role of TRAP220 in the TRAP/DRIP complex may account for the reported transcriptional squelching between ER and BRCA1. Indeed, several other BRCT-associated proteins we identified were also TRAP/DRIP complex components, such as TRAP220, TRAP240, DRIP130, and TRAP80 (Ito et al., 1999). BACH1 (Cantor et al., 2001) and p300 (Pao et al., 2000) were also detected by TOF-MAS and Western blotting (Figure 1b), respectively, and have been previously shown to interact with BRCT, which confirmed the efficacy of our purification method.

To address the functional importance of the BRCT-TRAP220 interaction, a BRCT point-mutant, derived from a breast cancer patient and deficient in transcriptional activity, was used to isolate interacting complexes. As clearly shown in Figure 3b, the GST-fused BRCT

point-mutant (M1775R) protein lacked the ability to retain TRAP220 on the column. This indicated that TRAP220 may function as a co-activator in the BRCA1 complex. To determine whether full-length BRCA1 protein interacted with TRAP220 in human cells, we expressed full-length BRCA1 (FLAG epitope-tagged) and/or TRAP220 (His/Myc epitope-tagged) in 293T cells. Significant expression of the tagged proteins was confirmed by Western blotting. After immunoprecipitation with anti-FLAG M2 to obtain full-length BRCA1, the immunoprecipitants were blotted with anti-Myc to identify TRAP220-containing complexes (Figure 2a). Both TRAP220 and BRCA1 were detected in cell lysate immunoprecipitates (Figure 2a), which supported the hypothesis that BRCA1 physically associates with TRAP220 in living cells. This hypothesis was further confirmed by in vivo association between endogenous BRCA1 and TRAP220 in MCF-7 cells expressing both proteins (Figure 2b). No such association was observed when the BRCA1 point-mutant (M1775R) was used instead of wild-type BRCA1 in the immunoprecipitation experiment (Figure 2a), as expected from the results of the column purification experiments.

To map the region of TRAP220 that interacted with BRCT, a GST pull-down assay was performed using TRAP220 deletion mutants (Figure 3a). FLAG-tagged TRAP220 fragments, abbreviated TR1, TR2, TR3, TR4 and TR5 (as described in Figure 3a), were in vitro translated in the presence of [³⁵S]methionine and incubated with GST-fused BRCT protein-bound resin. Only TR1 was trapped, which suggested that only the TR1 region interacted with BRCT. Interestingly, the
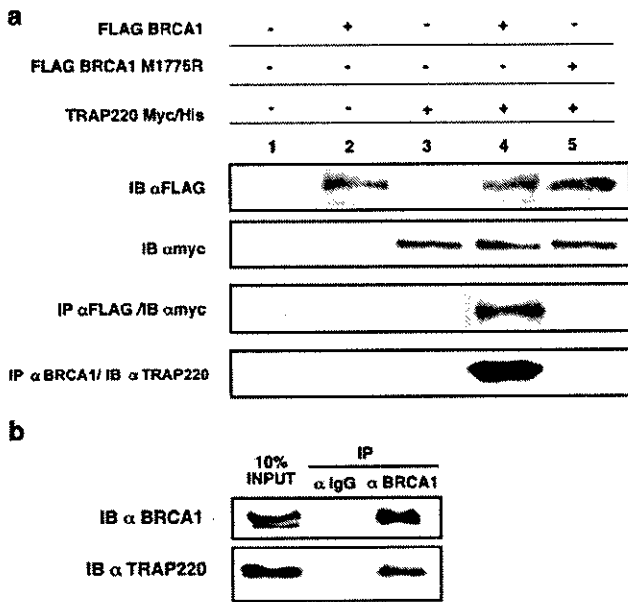
6002

**a**



**b**



Figure 2 *In vivo* association between TRAP220 and BRCA1. (a) Formation of BRCA1 and TRAP220 complexes in 293T cells was analysed by co-immunoprecipitation (IP) using the anti-FLAG monoclonal M2 antibody (Sigma Aldrich) followed by immuno-blotting (IB) using anti-Myc. 293T cells were transiently transfected with combinations of expression vectors as indicated. The expression of proteins in transfected cell extracts was determined by Western blot analysis using FLAG or Myc tags. (b) Detection of endogenous BRCA1-TRAP220 interaction by Western blotting. MCF-7 nuclear extracts were applied for immunoprecipitation with 5 μg of anti-BRCA1 (MS-BRC14-UP50, GeneTex, Inc.) and IgG, respectively. Then bound proteins in 30 μl of protein G sepharose™ 4 Fast Flow (Amersham Biosciences, NJ, USA) were detected by Western blotting. The 10% amount of the tested nuclear extracts is shown as positive control as input (Kitagawa *et al.*, 2003)

BRCT column did not retain either TR2 or TR3, which contain LXXLL motifs thought to interact with liganded NRs. Reflecting the associations between TRAP220 and wild-type or point-mutant BRCA1 as observed in our *in vivo* experiments, the point-mutations A1708E, P1749R, and M1775R that exhibit no BRCA1 transactivation function caused the loss of TRAP220 interaction *in vitro* (Figure 3b).

To examine the co-activator activity of TRAP220 toward BRCT transactivation function, a transient transfection assay was performed using a luciferase reporter plasmid driven by the adenovirus major late promoter (AdMLP) containing GAL4DBD-binding sites. A BRCT-GAL4DBD-fusion protein (GAL-BRCT) alone potently stimulated transcription (Figure 4b). TRAP220 expression in human 293T cells led to an approximately twofold increase in luciferase activity compared to GAL-BRCT alone, while such co-activation was not detected in a TRAP220 deletion mutant lacking the BRCT interacting TR1 region (amino acids 1–326, see Figure 3a) (Figure 4b). This enhancement of transactivation by TRAP220 was not observed when either GAL4 DNA-binding domain alone or GAL-BRCT mutants (A1708E, P1749R, or M1775R) were used, as expected from the *in vivo* and *in vitro* TRAP220 experiments. Consistent with these findings, antisense TRAP220 expression, that disrupted endogenous TRAP220 expression (Figure 4a), reduced the transcriptional activity of BRCT (Figure 4b). This again suggested a significant role for TRAP220 in BRCA1 transactivation function.

Finally, we then tested the significance of TRAP220 activity in the DNA damage response mediated by BRCA1. BRCA1 was transfected into HCC1937 cells (a
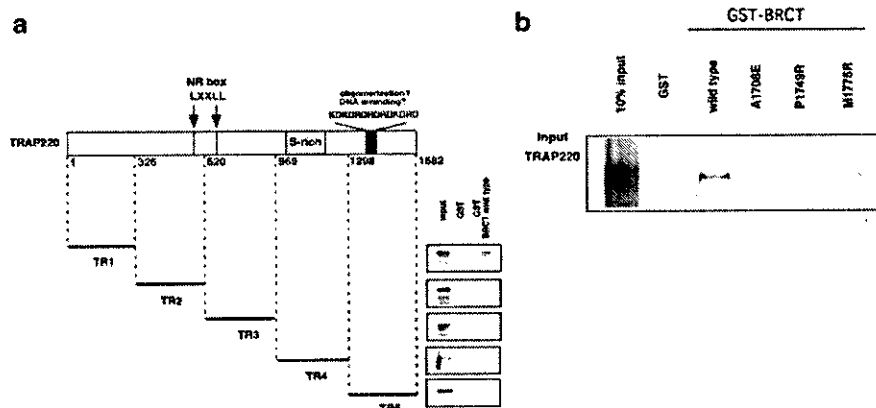
**a**



**b**



Figure 3 *In vitro* association between TRAP220 and BRCT, and mapping of the BRCT-interacting region of TRAP220. (a) Mapping of the BRCT-interacting region of TRAP220 using GST-BRCT and TRAP220 fragments. Bacterially expressed GST-fusion proteins immobilized on beads were used in *in vitro* pull-down assays. A schematic diagram of the structure of TRAP220 is shown. TRAP220 'TR1' (amino acids 1–326), 'TR2' (326–620), 'TR3' (620–969), 'TR4' (969–1298), and 'TR5' (1298–1582) were *in vitro* translated in the presence of [³⁵S]methionine (Amersham Pharmacia Biotech) using a TNT coupled *in vitro* translation system (Promega). Each labelled TRAP220 fragment was then incubated with either GST alone or GST-BRCT. The mixtures were washed and subjected to SDS–PAGE and analysed. Polyacrylamide gels were stained briefly with Coomassie Brilliant Blue to verify the loading of equal amounts of fusion proteins prior to drying and autoradiography (Ohtake *et al.*, 2003). (b) *In vitro* association of TRAP220 with BRCT or BRCT point mutants that lack transcriptional activity were performed by incubating GST, GST-BRCT, GST-BRCT A1708E, P1749R, or M1775R with *in vitro* translated TRAP220
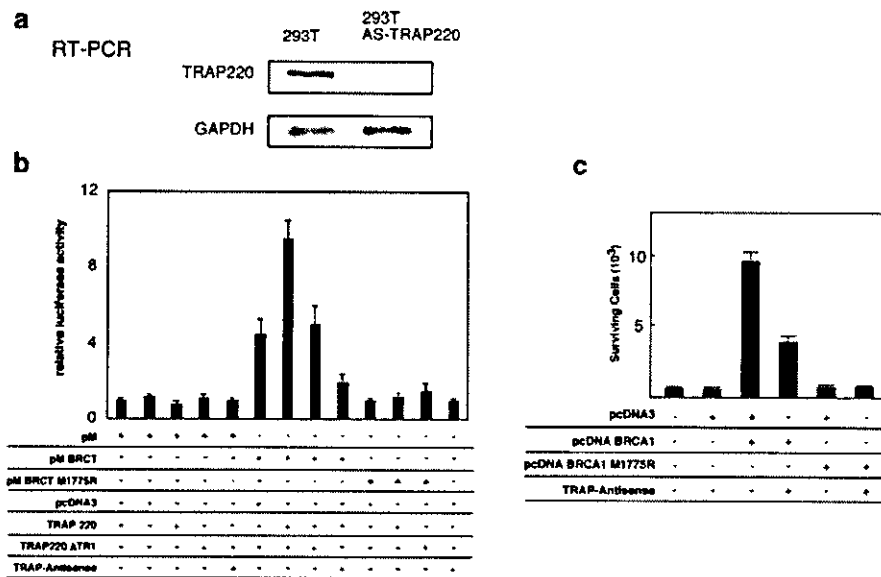
**Figure 4** TRAP220 activates transcription by GAL-BRCT, while antisense TRAP220 disrupts the DNA damage response of BRCA1. (a) Transfection of antisense TRAP220 in 293T cells reduced TRAP220 expression as shown by RT-PCR analysis. (b) Transient transfection assays of GAL-BRCT and FLAG-TRAP220 using a luciferase reporter (Promega) containing the GAL4 DNA-binding site (17M8) showed specific enhancement of transcription. 293T cells were transfected with each luciferase reporter (Elb-Luc and AdMLP-Luc), pM or pM-BRCT, pRL CMV-Luc as a control of transfection efficiency, and either pcDNA3 (Invitrogen) empty expression vector, pcDNA FLAG-TRAP220, pcDNA TRAP220ΔTR1 or antisense TRAP220. Measurements of luciferase (Promega) activity were performed according to the manufacturer's instructions. Error bars indicate the standard deviation. Each experiment was repeated at least three times in triplicate (Watanabe et al., 2001). (c) HCC1937 cells were transfected with constructs based on the pcDNA3 plasmid. Cultures were treated with 0.1% MMS for 50 min, and surviving cells were counted after 8 days, as previously described by Zhong et al. (1999)

mutated BRCA1 cell line) that are hypersensitive to DNA damaging agents such as methylmethane sulfonate (MMS). By counting the number of surviving HCC1937 cells, we observed a protective effect of BRCA1 expression in response to DNA damage. Antisense TRAP220 expression resulted in specific deterioration in the DNA damage response potentiated by BRCA1 (Figure 4c), which verified the importance of TRAP220 in BRCA1 function.

BRCA1 is a multifunctional protein that acts as a tumor suppressor controlling gene expression, as well as a sequence-specific regulator and a co-regulator controlling DNA damage (Venkitaraman, 2002). Therefore, it can be speculated that BRCA1 acts as a platform protein that associates with a number of factors, regulators, and complexes to accomplish the diverse functions attributed to BRCA1. Indeed, discrete classes of factors and complexes involved in gene regulation and DNA repair associated with BRCA1 have been identified, and indirect associations with further related factors and complexes are supposed. Nevertheless, clear relationships between *BRCA1* gene mutation and consequent malfunctions of the identified factors and complexes remain to be established. To this end, we searched for co-activator complexes that recognized the BRCT domain, as mutations in this domain modulate BRCA1 transactivation function and are highly related with breast and ovarian cancer incidence (Humphrey et al., 1997; Greenman et al., 1998). Also, a previous

report found that BRCA1 competed with ER in terms of transcriptional control via the BRCT domain, which suggested the possibility of common co-activator complexes between ER and BRCA1, presumably including the TRAP/DRIP complex already identified as an ER co-activator complex (Ito et al., 1999; Rachez et al., 1999; Yanagisawa et al., 2002).

In this study based on biochemical approaches (Yanagisawa et al., 2002; Kitagawa et al., 2003), we showed that a TRAP220-containing complex associated with wild-type BRCT through physical interaction with TRAP220. As TRAP220 binding of BRCA1 was abrogated in vivo and in vitro when clinically relevant BRCA1 mutants that lacked transactivation function (Chapman and Verma, 1996) were used as bait, the association between BRCT and TRAP220 complexes appears to be critical for normal BRCA1 function. This is supported by the findings that TRAP220 alone potently enhanced BRCA1 transactivation function, and that the disruption of endogenous TRAP220 by antisense TRAP220 led to a clear reduction in BRCA1-mediated DNA damage repair. This last result suggested that TRAP220-containing complexes may also play a role in the DNA damage repair function of BRCA1.

The TRAP/DRIP mediator complex was originally isolated as a co-activator complex for different classes of activators, including NRs, by several independent groups (Fondell et al., 1996; Rachez et al., 1999). Further study of the isolated complex components

revealed that the complexes formed a class of co-activator complexes that shared common major components along with limited numbers of specific factors (Gu et al., 1999). Combinations of these specific components generate a number of TRAP/DRIP complex subclasses (Freedman, 1999). The co-activator function of TRAP/DRIP complexes in in vitro transcription systems illustrates the direct link of the activator complex to the basal transcription machinery. The 220-kDa component of the complex, referred to as TRAP220/DRIP230, was identified as a subunit with unique properties in that it directly binds to NRs in a ligand-dependent manner through a region containing NR recognition motifs (LXXLL, NR box) (Ito et al., 1999; Rachez et al., 1999). Given that BRCA1 may compete with ER with respect to gene regulation, and that mutations in the BRCT region lead altered BRCA1-dependent gene regulation and enhanced tumorigenesis in estrogen-dependent cancers (presumably through modulation of ER-mediated estrogen signaling), interaction between TRAP220 and BRCA1 may account for the transcriptional squelching observed between BRCA1 and ER (Fan et al., 1999; Zheng et al., 2001).

The results of our study showed that TRAP220 bound directly to wild-type BRCA1, but not to BRCA1 mutants. Thus, breast cancer predisposition caused by genetic mutations in the BRCT domain may be due, at least in part, to insufficient interaction with TRAP

complexes. In this respect, it is perhaps surprising that gene amplification or overexpression of TRAP220 is observed in some cancer cell lines (Zhu et al., 1999). Our transient transfection assay showed that TRAP220 enhanced BRCT-mediated transactivation function, such that the TRAP complex clearly served as a co-activator complex in the promoters of BRCA1 target genes. In conclusion, we propose that the failure of binding between BRCT and TRAP220 is a key event in cancer predisposition. Further investigations should be performed to elucidate the molecular mechanisms that underlie the formation BRCA1-TRAP complexes in normal cell growth, thereby revealing its role as a tumor suppressor in estrogen-responsive organs, especially the breast and ovary.

## Abbreviations

BRCA1, breast cancer susceptibility gene 1; GST, glutathione S-transferase; CMV, cytomegalovirus; AdMLP, adenovirus major late promoter; NR, nuclear receptor.

## References

Anderson SF, Schlegel BP, Nakajima T, Wolpin ES and Parvin JD. (1998). Nat. Genet., 19, 254–256.

Bochar DA, Wang L, Beniya H, Kinev A, Xue Y, Lane WS, Wang W, Kashanchi F and Shiekhattar R. (2000). Cell, 102, 257–265.

Callebaut I and Mornon JP. (1997). FEBS Lett., 400, 25–30.

Cantor SB, Bell DW, Ganesan S, Kass EM, Drapkin R, Grossman S, Wahrer DC, Sgroi DC, Lane WS, Haber DA and Livingston DM. (2001). Cell, 105, 149–160.

Chapman MS and Verma IM. (1996). Nature, 382, 678–679.

Fan S, Wang J, Yuan R, Ma Y, Meng Q, Erdos MR, Pestell RG, Yuan F, Auborn KJ, Goldberg ID and Rosen EM. (1999). Science, 284, 1354–1356.

Fondell JD, Ge H and Roeder RG. (1996). Proc. Natl. Acad. Sci. USA, 93, 8329–8333.

Fondell JD, Guermah M, Malik S and Roeder RG. (1999). Proc. Natl. Acad. Sci. USA, 96, 1959–1964.

Freedman LP. (1999). Cell, 97, 5–8.

Futreal PA, Liu Q, Shattuck-Eidens D, Cochran C, Harshman K, Tavtigian S, Bennett LM, Haugen-Strano A, Swensen J, Miki Y, Eddington K, McClure M, Frye C, Weaver-Feldhaus J, Ding W, Gholami Z, Söderkrist P, Terry L, Jhanwar S, Berchuck A, Iglehart JD, Marks J, Ballinger DG, Barrett JC, Skolnick MH, Kamb A and Wiseman R. (1994). Science, 266, 120–122.

Greenman J, Mohammed S, Ellis D, Watts S, Scott G, Izatt L, Barnes D, Solomon E, Hodgson S and Mathew C. (1998). Genes Chromosomes Cancer, 21, 244–249.

Gu W, Malik S, Ito M, Yuan CX, Fondell JD, Zhang X, Martinez E, Qin J and Roeder RG. (1999). Mol. Cell., 3, 97–108.

Humphrey JS, Salim A, Erdos MR, Collins FS, Brody LC and Klausner RD. (1997). Proc. Natl. Acad. Sci. USA, 94, 5820–5825.

Ito M, Yuan CX, Malik S, Gu W, Fondell JD, Yamamura S, Fu ZY, Zhang X, Qin J and Roeder RG. (1999). Mol. Cell., 3, 361–370.

Kawai H, Li H, Chun P, Avraham S and Avraham HK. (2002). Oncogene, 21, 7730–7739.

Kitagawa H, Fujiki R, Yoshimura K, Mezaki Y, Uematsu Y, Matsui D, Ogawa S, Unno K, Okubo M, Tokita A, Nakagawa T, Ito T, Ishimi Y, Nagasawa H, Matsumoto T, Yanagisawa J and Kato S. (2003). Cell, 113, 905–917.

Mangelsdorf DJ, Thummel C, Beato M, Herrlich P, Schutz G, Umesono K, Blumberg B, Kastner P, Mark M, Chambon P and Evans RM. (1995). Cell, 83, 835–839.

Miki Y, Swensen J, Shattuck-Eidens D, Futreal PA, Harshman K, Tavtigian S, Liu Q, Cochran C, Bennett LM, Ding W, Bell R, Rosenthal J, Hussey C, Tran T, McClure M, Frye C, Hattier T, Phelps R, Haugen-Strano A, Katcher H, Yakumo K, Gholami Z, Shaffer D, Stone S, Bayer S, Wray C, Bogden R, Dayananth P, Ward J, Tonin P, Narod S, Bristow PK, Norris FH, Helvering L, Morrison P, Rosteck P, Lai M, Barrett JC, Lewis C, Neuhausen S, Cannon-Albright L, Goldgar D, Wiseman R, Kamb A and Skolnick MH. (1994). Science, 266, 66–71.

Miyake T, Hu YF, Yu DS and Li R. (2000). J. Biol. Chem., 275, 40169–40173.

Monteiro AN, August A and Hanafusa H. (1996). Proc. Natl. Acad. Sci. USA, 93, 13595–13599.

Moynahan ME, Chiu JW, Koller BH and Jasin M. (1999). Mol. Cell., 4, 511–518.

6005

Ohtake F, Takeyama K, Matsumoto T, Kitagawa H, Yamamoto Y, Nohara K, Tohyama C, Krust A, Mimura J, Chambon P, Yanagisawa J, Fujii-Kuriyama Y and Kato S. (2003). *Nature*, **423**, 545–550.

Pao GM, Janknecht R, Ruffner H, Hunter T and Verma IM. (2000). *Proc. Natl. Acad. Sci. USA*, **97**, 1020–1025.

Rachez C, Lemon BD, Suldan Z, Bromleigh V, Gamble M, Naar AM, Erdjument-Bromage H, Tempst P and Freedman LP. (1999). *Nature*, **398**, 824–828.

Scully R, Ganesan S, Vlasakova K, Chen J, Socolovsky M and Livingston DM. (1999). *Mol. Cell.*, **4**, 1093–1099.

Venkitaraman AR. (2002). *Cell*, **108**, 171–182.

Watanabe M, Yanagisawa J, Kitagawa H, Takeyama K, Ogawa S, Arao Y, Suzawa M, Kobayashi Y, Yano T, Yoshikawa H, Masuhiro Y and Kato S. (2001). *EMBO J.*, **20**, 1341–1352.

Yanagisawa J, Kitagawa H, Yanagida M, Wada O, Ogawa S, Nakagomi M, Oishi H, Yamamoto Y, Nagasawa H, McMahon SB, Cole MD, Tora L, Takahashi N and Kato S. (2002). *Mol. Cell.*, **9**, 553–562.

Yarden RI and Brody LC. (1999). *Proc. Natl. Acad. Sci. USA*, **96**, 4983–4988.

Yu X, Wu LC, Bowcock AM, Aronheim A and Baer R. (1998). *J. Biol. Chem.*, **273**, 25388–25392.

Zhang H, Somasundaram K, Peng Y, Tian H, Bi D, Weber BL and El-Deiry WS. (1998). *Oncogene*, **16**, 1713–1721.

Zheng L, Annab LA, Afshari CA, Lee WH and Boyer TG. (2001). *Proc. Natl. Acad. Sci. USA*, **98**, 9587–9592.

Zhong Q, Chen CF, Li S, Chen Y, Wang CC, Xiao J, Chen PL, Sharp ZD and Lee WH. (1999). *Science*, **285**.

Zhu Y, Qi C, Jain S, Le Beau MM, Espinosa III R, Atkins GB, Lazar MA, Yeldandi AV, Rao MS and Reddy JK. (1999). *Proc. Natl. Acad. Sci. USA*, **96**, 10848–10853.

IV - 125

# In vivo potentiation of human oestrogen receptor α by Cdk7-mediated phosphorylation

Saya Ito[1], Ken-ichi Takeyama[1,2], Ayako Yamamoto[1], Shun Sawatsubashi[1], Yuko Shirode[1,2], Alexander Kouzmenko[1,2], Tetsuya Tabata[1] and Shigeaki Kato[1,2,*]

[1]The Institute of Molecular and Cellular Biosciences, University of Tokyo, Bunkyo-ku, Tokyo, Japan
[2]SORST, Japan Science and Technology, Kawaguchi, Saitama, Japan

Phosphorylation of the Ser[118] residue in the N-terminal A/B domain of the human oestrogen receptor α (hERα) by mitogen-activated protein kinase (MAPK), stimulated via growth factor signalling pathways, is known to potentiate ERα ligand-induced transactivation function. Besides MAPK, cyclin dependent kinase 7 (Cdk7) in the TFIIH complex has also been found to potentiate hERα transactivation in vitro through Ser[118] phosphorylation. To investigate an impact of Cdk7 on hERα transactivation in vivo, we assessed activity of hERα in a wild-type and cdk7 inactive mutant Drosophila that ectopically expressed hERα in the eye disc. Ectopic expression of the wild-type or mutant receptors, together with a green fluorescent protein (GFP) reporter gene, allowed us to demonstrate that hERα expressed in the fly tissues was transcriptionally functional and adequately responded to hERα ligands in the patterns similar to those observed in mammalian cells. Replacement of Ser[118] with alanine in hERα (S118A mutant) significantly reduced the ligand-induced hERα transactivation function. Importantly, while in cdk7 inactive mutant Drosophila the wild-type hERα exhibited reduced response to the ligand; levels of transactivation by the hERα S118A mutant were not affected in these inactive cdk7 mutant flies. Furthermore, phosphorylation of hERα at Ser[118] has been observed in vitro by both human and Drosophila Cdk7. Our findings demonstrate that Cdk7 is involved in regulation of the ligand-induced transactivation function of hERα in vivo via Ser[118] phosphorylation.

## Introduction

It is thought that most of the wide variety of oestrogen action is mediated through the transcriptional control of target genes by nuclear oestrogen receptor (ER) (Couse & Korach 1999; Ciana et al. 2003). The two subtypes of ER, α and β, belong to the nuclear receptor superfamily and act as ligand-induced transcription factors. As in other nuclear receptor superfamily members, structure of ER proteins is divided into five or six functional domains (designated as A to E/F domains). The highly conserved DNA binding domain is located in the C domain, while the ligand-binding domain (LBD) is mapped to the E/F domain. Transactivation function is present in the N-terminal A/B domain (AF-1) and in the C-terminal LBD (AF-2) (Kumar et al. 1987; Tora et al. 1989). Although both AF-1 and AF-2 are involved in the

ligand-dependent transactivation function of ERs, AF-1 is constitutively active, while AF-2 activity is dependent on ligand binding (Endoh et al. 1999; Kobayashi et al. 2000; Watanabe et al. 2001). AF-1 and AF-2 domains have distinctive properties and their activities may depend on cell type and promoter context (Kumar et al. 1987; Tora et al. 1989).

ER target gene promoters contain oestrogen-response elements (EREs) that are recognized and directly bound by ER homo- or hetero-dimers followed by chromatin remodelling, presumably by recruited ATP-dependent chromatin remodelling complexes (Belandia & Parker 2003; Kitagawa et al. 2003). ERE-bound liganded ERs also induce recruitment of a number of histone acetyl-transferase (HAT) and non-HAT cofactors that activate transcription (McKenna & O'Malley 2002). HAT coactivator complexes, CBP/p160 (Onate et al. 1995; Kamei et al. 1996; Chen et al. 1997; Spencer et al. 1997) and TRRAP/GCN5 (Yanagisawa et al. 2002), and non-HAT DRIP/TRAP complexes (Fondell et al. 1996;

Yuan *et al.* 1998; Naar *et al.* 1999; Rachez *et al.* 1999) are thought to act as common coactivator complexes for ERs as well as for other DNA-binding transcription factors. Therefore, ligand binding leads to structural alteration and switch of ER function from transcriptional repression to transcriptional activation via the recruitment of coactivators (Shiau *et al.* 1998; Freedman 1999; Glass & Rosenfeld 2000; Metivier *et al.* 2003).

It is well known that phosphorylation of ERα modulates the activity of both AF-1 and AF-2 (Ali *et al.* 1993; Le *et al.* 1994; Kato *et al.* 1995; Chen *et al.* 2000). Among sites of potential phosphorylation, Ser[118] residue (S118) in the hERα AF-1 domain has been particularly intensively studied with regard to the state of its phosphorylation and consequent potentiation of AF-1 activity. We have previously demonstrated that Ser[118] is phosphorylated by ERK, a MAPK activated by the epidermal growth factor (EGF) or insulin-like growth factor (IGF) signalling, that results in the AF-1 potentiation in cultured cells (Kato *et al.* 1995). More recently, Chen and colleagues have shown that Cdk7 also phosphorylates hERα Ser[118] in an oestrogen-dependent manner and enhances ERα transactivation in mammalian cells in culture (Chen *et al.* 2000). As Cdk7 is a key subunit of the basal transcription factor TFIIH complex (Frit *et al.* 1999; Egly 2001), it has been suggested that this phosphorylation takes place when TFIIH is recruited adjacent to hERα, presumably in the transcription initiation complex. Therefore, accumulating evidence suggests that phosphorylation of hERα Ser[118] may play a significant role in regulation of AF-1 activity. However, the physiological role of Ser[118] phosphorylation and associated kinases in hERα function remain to be established *in vivo*.

In *Drosophila melanogaster*, at least 20 members of the nuclear receptor (NR) family, such as the ecdysone receptor (EcR), have been genetically identified that, similar to the vertebrate NRs, are thought to transcriptionally control expression of target genes (Talbot *et al.* 1993; Baker *et al.* 2003). Recently, we reported that human androgen receptor ectopically expressed in *Drosophila* tissues was transcriptionally active and responsive to AR agonists and antagonists (Takeyama *et al.* 2002). In the present study, to assess an impact of Ser[118] phosphorylation by Cdk7 and related kinases on hERα activity *in vivo*, we generated transgenic *Drosophila* lines in which hERα was ectopically expressed in specific *Drosophila* tissues using a GAL4/UAS system (Brand & Perrimon 1993). hERα expressed in the fly was transcriptionally functional and responded adequately to ER ligands, as expected from mammalian studies. Apparently, for its transactivation function in these transgenic flies, hERα recruited endogenous co-activators, such as those shown to be homologous to

mammalian CBP and AIB1 (Akimaru *et al.* 1997; Bai *et al.* 2000). We found that replacement of S118 with alanine residue (S118A) in hERα resulted in the marked reduction of ligand-induced hERα transactivation in transgenic fly eye disc. Furthermore, in a *cdk7* inactive mutant *Drosophila* (*cdk7*[a]) (Larochelle *et al.* 2001), transactivation by the wild-type but not the S118A hERα was significantly reduced. In addition, both human and *Drosophila* recombinant Cdk7 were equally able to phosphorylate hERα at Ser[118] *in vitro*. We have also shown that Cdk7 acts as a co-activator of hERα transactivation in transfected cells in culture. Therefore, our results provide for the first time genetic evidence that phosphorylation of Ser[118] potentiates transcriptional activity of hERα and that Cdk7 is involved in regulation of the ligand-induced transactivation function of hERα *in vivo* through Ser[118] phosphorylation.

## Results

### hERα in *Drosophila* is transcriptionally functional

Our previous studies showed that human androgen receptor ectopically expressed in *Drosophila* tissues was adequately functional (Takeyama *et al.* 2002). We have utilized the same strategy to generate transgenic *Drosophila* expressing hERα together with ERE-dependent green fluorescent protein (GFP) as a reporter gene. Wild-type hERα (HEG0), AF-1 (HE15) or AF-2 (HE19) domains (as illustrated in Fig. 1A) were ectopically expressed in photoreceptor cells under control of the glass multimer reporter (*GMR*) gene promoter (Moses & Rubin 1991) using the *Drosophila melanogaster GAL4-UAS* system (Brand & Perrimon 1993). The eye disc, one of several larval discs in *Drosophila*, has been shown to be an effective model to assess Cdk7 function as a cell survival signal. Expression of hERα proteins was estimated by staining with immunofluorescent antibody. Levels of GFP reporter expression in respective eye discs were quantified by green fluorescence and normalized against the levels of ERα protein to determine fold of activation.

Dietary administration of 17β-oestradiol (E2) for 5 days from hatching remarkably induced GFP expression (Fig. 1B). The partial oestrogen agonist tamoxifen (TAM) and pure antagonist ICI182.780 exhibited partial oestrogenic and anti-oestrogenic actions, respectively, similar to that observed in mammals (McDonnell *et al.* 1995). E2-dependent (AF-2) and -independent (AF-1) transactivation functions were observed in the C-terminal-LBD and N-terminal A/B domain expressing transgenic flies, respectively, as expected from previous studies (Kumar *et al.* 1987; Tora *et al.* 1989; Kobayashi *et al.* 2000; Watanabe
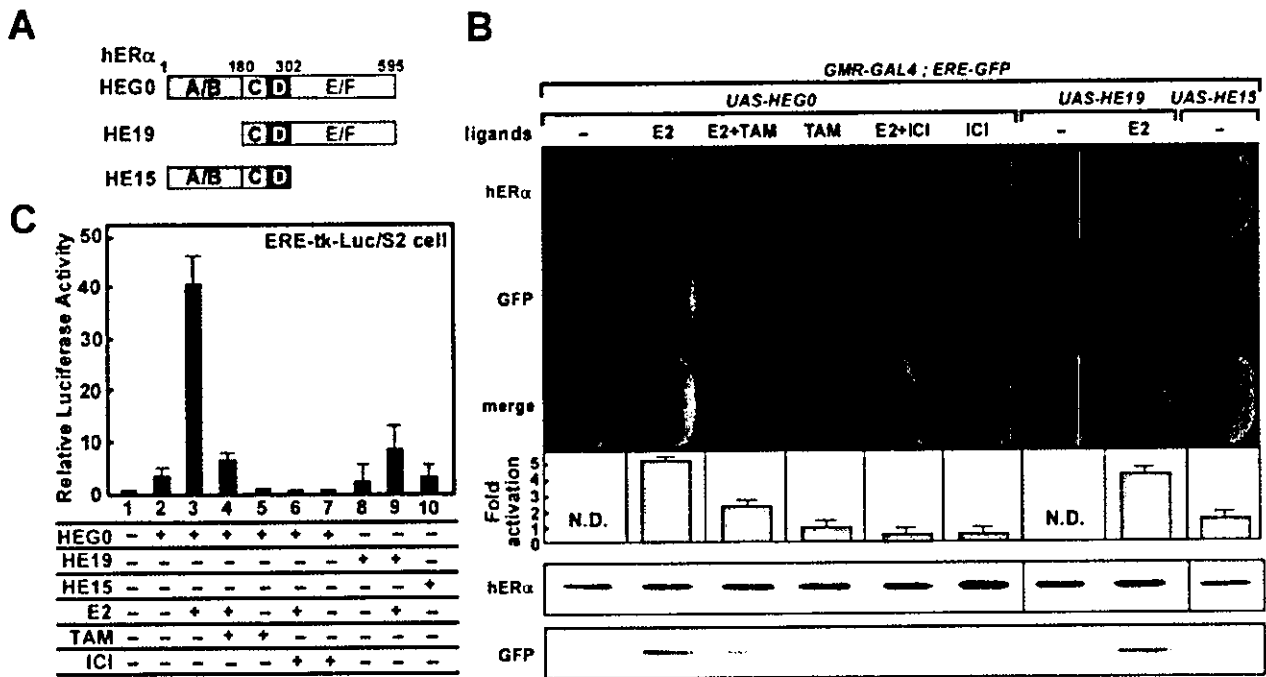
**A**



**B**



**C**



Figure 1 Ligand dependent transactivation of hERα in *Drosophila*. (A) Schematic representation of hERα constructs.The DNA binding domain (DBD) is located in the C domain (grey box).The transactivation function-1 (AF-1) region is located in the N-terminal A/B domain (blue box), while the transactivation function-2 (AF-2) region is located in the C-terminal E/F domain (white box) that also contains the ligand binding domain (LBD). (B) Ligand-dependent transactivation of hERα mutants in eye imaginal discs. Expression of hERα mutants in third instar larva eye discs driven by GMR-GAL4 was detected with ERα antibodies (B10 or HC-20) (red). Transactivation of hERα mutants was estimated by GFP expression (green).The anterior is to the right. Bottom panels: hERα and GFP expression in four pairs of adult heads as detected by Western blotting. Fold-activation was calculated using hERα expression levels as normalizing factor. Ligands, $10^{-3}$ M 17β-oestradiol (E2), $10^{-2}$ M tamoxifen (TAM), and $10^{-2}$ M ICI 182.780 (ICI), were added in 100 μL of vehicle on top of 10 mL of the medium before hatching. Flies were kept at 25 °C. (C) Measurement of hERα mutants transactivation in Schneider cells. Schneider cells were transfected with hERα mutant expression plasmids, Actin-GAL4 plasmid, ERE-tk-luc reporter plasmid and pRL-CMV internal control plasmid in the presence or absence of $10^{-8}$ M E2, $10^{-8}$ M TAM or $10^{-8}$ M ICI. Firefly luciferase activity (ERE-tk-luc) was measured and normalized against Renilla activity (pRL-CMV-luc) as an internal control. Data are shown as the average and standard deviation of three independent experiments.

*et al.* 2001). Similar hER ligand effects and hERα AF-1 and AF-2 activities were observed in Schneider (S2) cells derived from *Drosophila* embryos (Fig. 1C).These data indicated that hERα ectopically expressed in *Drosophila* tissues was adequately functional in ligand-induced transactivation, presumably through recruitment of endogenous co-regulators. Therefore, it appears that human steroid receptors ectopically expressed in *Drosophila* retain their transactivation function.

## Co-activation of hERα by *Drosophila* CBP and p160 HAT homologues

As hERα was transcriptionally functional in insect cells in culture and in *Drosophila* eye disc cells *in vivo*, ability of endogenous fly co-activators to modulate hERα

transactivation was assessed in mutant flies deficient for *Drosophila* homologues of mammalian p160 (*tai*) or CBP (*nej*) (Akimaru *et al.* 1997; Bai *et al.* 2000).The oestrogen-induced transactivation function of hERα was clearly reduced in both of these mutants without affecting levels of hERα expression (Fig. 2).These data suggest that *Drosophila* homologue of the mammalian p160/CBP HAT complex acts as a co-activator of hERα in the fly cells. This was further confirmed by the observation of enhanced hERα transactivation in flies over-expressing TAI, *Drosophila* AIB1 homologue, in the eye disc.

The p160/CBP HAT complex has been shown to activate hERα AF-2 via the direct association of p160 family member proteins with helix 12 of the hERα LBD (Onate *et al.* 1995; Chen *et al.* 1997; Heery *et al.* 1997). However, little is known about the role of the
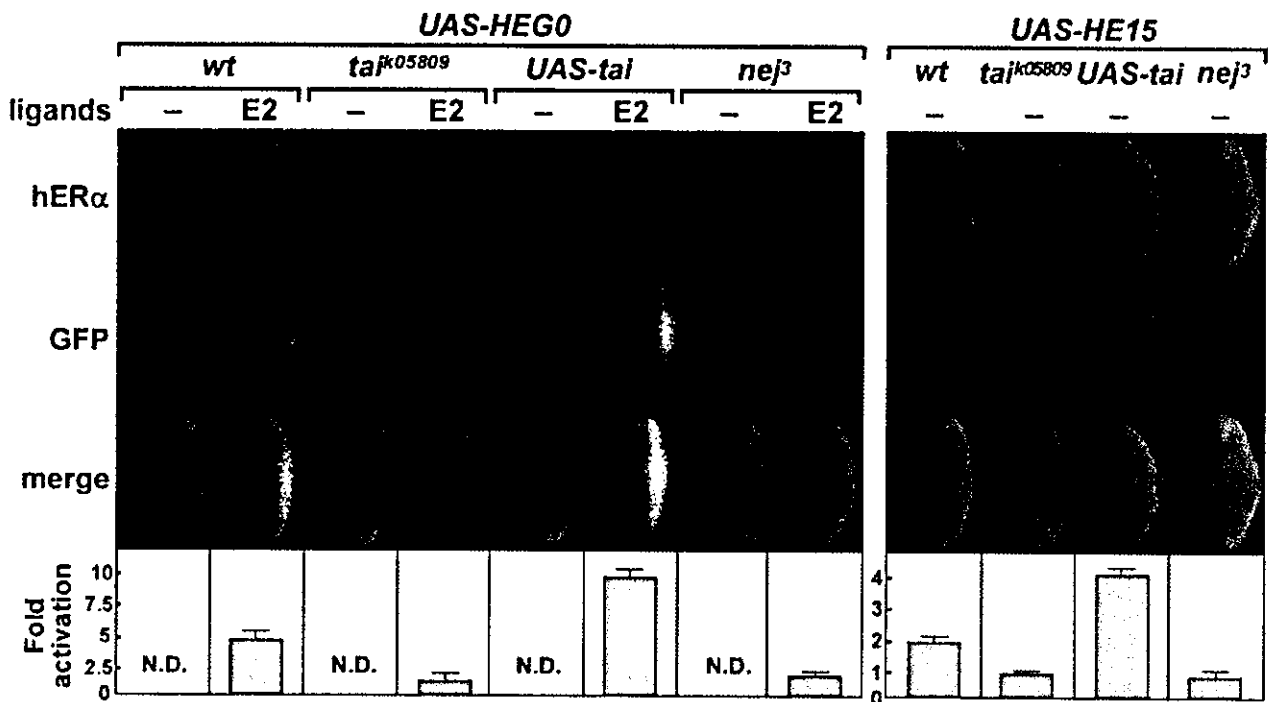
**Figure 2** hERα transactivation regulated by *Drosophila* transcriptional co-activators. hERα expression (red) and transactivation (green) were visualized by immunostaining with ERα antibodies (B10 and HC-20) and GFP expression, respectively, in eye imaginal discs. Fly lines contained single copies of *GMR-GAL4*, *UAS-hERα* (*HEG0* or *HE15*) and *ERE-GFP* with or without heterozygous *tai*[k05809], *UAS-tai* or *nej[3]*.

p160/CBP complex in modulation of hERα AF-1 activity. Although it is presumed that the complex bridges the AF-1 and AF-2 domains to synergistically enhance hERα transactivation function (Kobayashi *et al.* 2000), the p160/CBP complex was also able to enhance transcriptional activity of the AF-1 domain alone (i.e. the HE15 mutant). Indeed, similar patterns of AF-1 domain (HE15) and full-length hERα (HEG0) transactivation in mutant flies (Fig. 2) suggest that hERα AF-1 activity is modulated *in vivo* by the p160/CBP co-activator complex.

### Significant role of Ser[118] in hERα function *in vivo*

In mammalian cells, the potentiation of hERα AF-1 by phosphorylation of the Ser[118] residue has been well documented (Kato *et al.* 1995; Chen *et al.* 2000). However, the impact of Ser[118] phosphorylation in hERα transactivation function has not yet been verified *in vivo*. We tested the significance of hERα Ser[118] in the insect S2 cells transfected with hERα mutants containing a serine to alanine replacement at position 118 (HE457, HE15/457) (Fig. 3A and 3B). These mutants exhibited decreased transactivation capacities even though levels of the mutant expression appeared to be similar to that of wild-type hERα.

We then examined the role of Ser[118] in hERα function in transgenic flies (Fig. 3C). Although mutant and wild-type hERα expression levels in third instar larval eye discs were indistinguishable, a clear reduction in GFP induction was observed in the alanine replacement mutants. These findings provided evidence that the Ser[118] residue played a pivotal role in hERα transactivation *in vivo*.

### *In vivo* potentiation of hERα by Cdk7-mediated phosphorylation at Ser[118]

As it is likely that the Ser[118] residue could be phosphorylated by a number of endogenous protein kinases to support hERα transactivation, we studied the ability of dCdk7 to phosphorylate hERα at Ser[118] *in vitro* and *in vivo*. The serine/threonine kinase Cdk7 is indispensable for transcription initiation by RNA polymerase II as an essential component of the transcription factor TFIIH complex (Frit *et al.* 1999; Egly 2001). *dcdk7[s]* mutant flies express a temperature-sensitive Cdk7 mutant that is inactive at temperatures at or above 30 °C (Larochelle *et al.* 2001). We assessed transactivation function of HEG0 and HE457 in these *dcdk7[s]* mutant flies (Fig. 4, left panel). Oestrogen-induced transactivation of

**Figure 3** hERα transactivation is regulated by phosphorylation at Ser[118] in *Drosophila*. (A) Schematic representation of hERα mutant constructs. Ser[118] residue is the main phosphorylation site. (B) Transactivation of HEG0 and HE15 mutants in Schneider cells. Schneider cells were transfected with ERE-tk-luc reporter plasmid, Actin-GAL4 plasmid and each hERα mutants, and then incubated with or without $10^{-8}$ M E2. Luciferase activity data are shown as the average and standard deviation of three independent experiments. (C) Expression (red) and transactivation (green) of hERα mutants in eye imaginal discs. Fold-activation is represented as described (Fig. 1 legend). Genotypes are *GMR-GAL4/SM, UAS-hERα, ERE-GFP/TM3*.
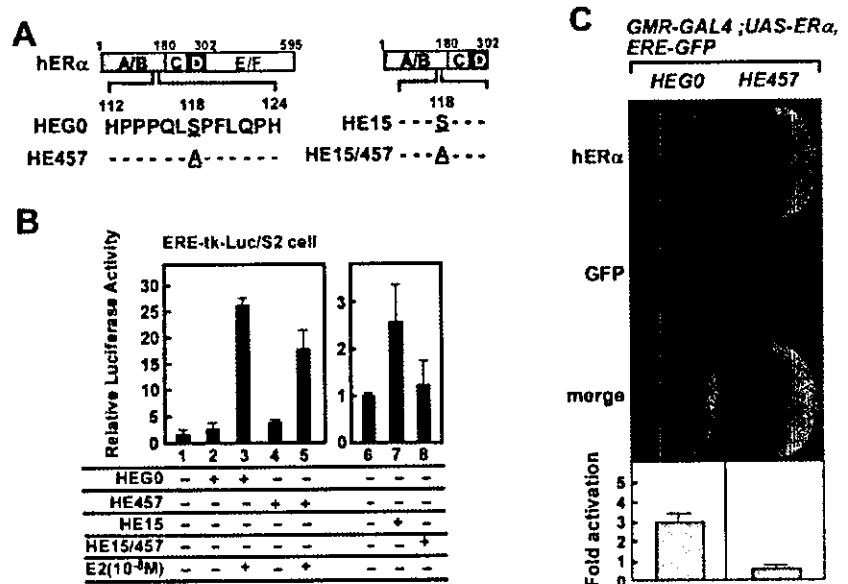


**Figure 4** hERα transactivation is enhanced by *Drosophila* Cdk7 through phosphorylation of Ser[118]. hERα expression (red) and trans-activation (green) in eye imaginal discs containing single copies of *GMR-GAL4, ERE-GFP* and *UAS-hERα (HEG0, HE457)* with or without heterozygous *cdk7⁵, cdk7⁶*, the temperature-sensitive *cdk7^{P140S}* gene, was introduced into the *Df(1)JB254-Pw⁺|snf⁺, dhd⁻| (cdk7*deficient) background. Flies were then incubated at 25 °C (room temperature) or 30 °C (h.s.) for 24 h in medium containing E2. GFP expression levels are represented as described.
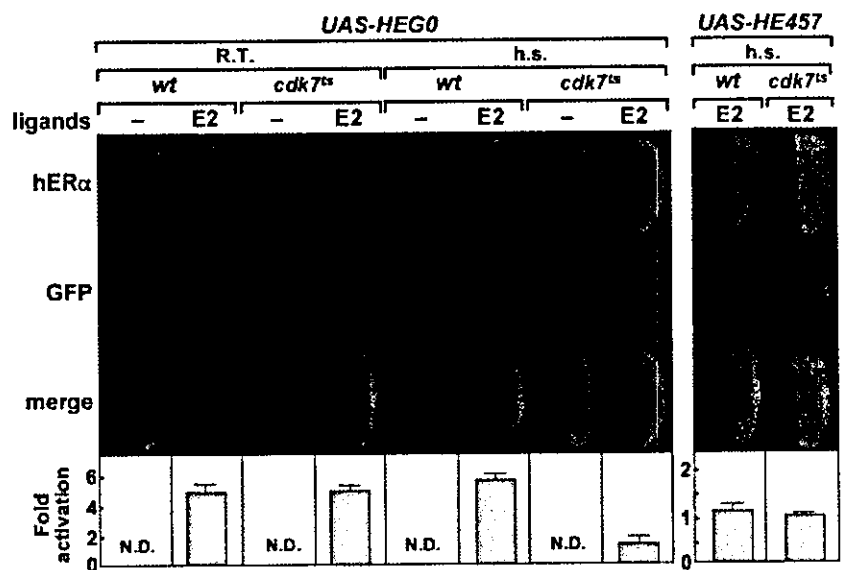


HEG0 in *dcdk7⁵* flies was significantly reduced at 30 °C in comparison with that at room temperature (25 °C). In contrast, HE457 transactivation in *dcdk7⁵* flies was not affected by exposure to high temperatures (Fig. 4, right panel). These results indicate that Cdk7 potentiated hERα transactivation *in vivo* through Ser[118] phosphorylation.

To further confirm this conclusion, we examined whether hERα Ser[118] is a substrate for dCdk7 *in vitro*. A recombinant GST-fused hERα segment (amino acids 56–180) chimera protein expressed in *E. coli*, and dCdk7 and hCdk7 expressed in 293T cells were used for the *in vitro* phosphorylation assay (Fig. 5A). GST-fused human

retinoic acid receptor α1 (hRARα1), a well-character-ized substrate for the mammalian Cdk7 (Rochette-Egly *et al.* 1997) was used as a positive control. dCdk7 and hCdk7 were equally capable of phosphorylating hERα and hRARα1. However, the Cdk7 phosphorylation was clearly reduced when the S118A mutant (HE457) was used as a substrate (Fig. 5B).

## Activation of the hERα S118A mutant by *Drosophila* AIB1 homologue

Finally, using a fly line with ectopical over-expression of *Drosophila* AIB1 homologue (TAI) in the eye disc, we
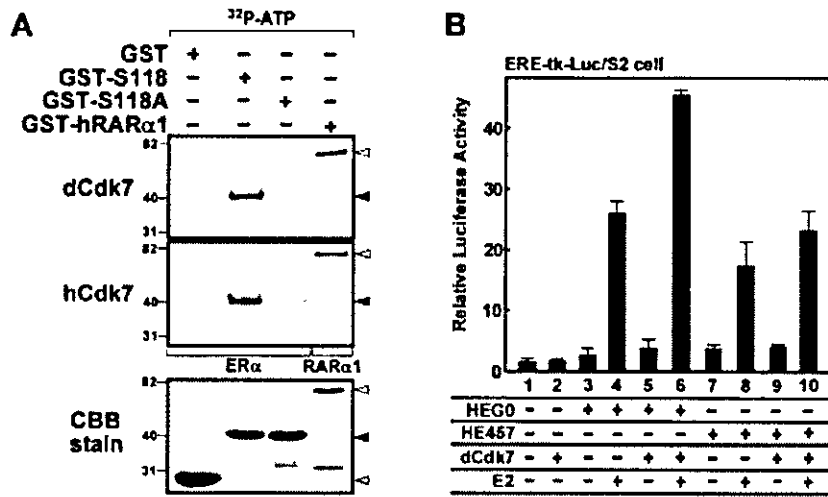
**A**



**B**



Figure 5 *In vitro* phosphorylation of hERα at Ser[118] by dCdk7. (A) Ten micrograms of GST-fused hERα (amino acids 56–180) and GST-fused hRARα1 were incubated with 9 µg dCdk7 or hCdk7. Phosphorylation and expression of GST-fused hERα amino acids (open arrow head), GST-fused hRARα1 (black arrow head), and GST (grey arrow head) were detected by autoradiography and CBB staining, respectively. (B) Schneider cells were co-transfected with 0.5 µg dCdk7 expression plasmid, 0.5 µg ERE-tk-luc reporter plasmid, 0.2 µg actin-GAL4 plasmid and hERα mutants and then incubated with or without 10⁻⁸ M E2. Luciferase activity data are shown as the average and standard deviation of three independent experiments.
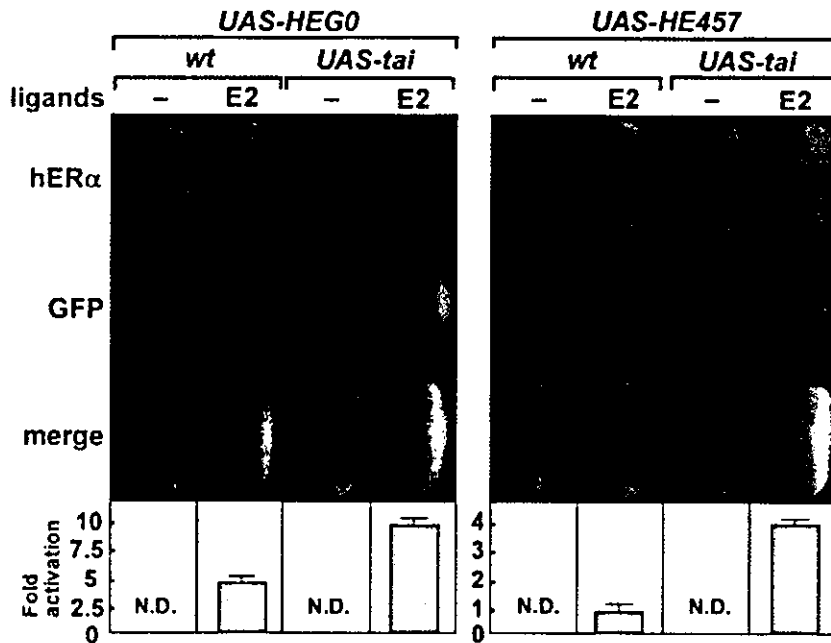


Figure 6 TAI enhancement of hERα transactivation is not dependent on Ser[118] phosphorylation status. hERα expression (red) and transactivation (green) in eye imaginal discs of either HEGO or HE457 expression lines are shown. TAI is also expressed driven by *GMR-GAL4*.

addressed a question whether enhancement of hERα transactivation by the p160/CBP complex is dependent on the receptor Ser[118] phosphorylation status. Although the hERα S118A mutant was less effective in the ligand-induced transactivation, TAI significantly enhanced transcriptional activity of both the mutant and the wild-type receptor (Fig. 6). This suggests that modulation of the ligand-induced hERα transactivation by the p160/CBP co-activator complex does not depend on the receptor phosphorylation.

## Discussion

### hERα expressed in *Drosophila* is functional in ligand-induced transactivation

We have previously shown that the human androgen receptor (hAR) ectopically expressed in *Drosophila* tissues was transcriptionally functional and responsive to hAR ligands similar to that in mammalian cultured cells and intact tissues (Takeyama *et al.* 2002). In the present study, we utilized the same approach and demonstrated